WSRC-MS-98-00604

Petrology and Geochemistry of Neoproterozoic Arc Plutons Beneath the Atlantic Coastal Plain, SRS, SC

by
M. Maryak
Westinghouse Savannah River Company
Savannah River Site
Aiken, South Carolina 29808
A. Dennis

A document prepared for JOURNAL ARTICLE: GEOLOGIC SOCIETY OF AMERICA at , , from - .

DOE Contract No. **DE-AC09-96SR18500**

DISCLAIMER

Petrology and Geochemistry of Neoproterozoic Arc Plutons Beneath the Atlantic Coastal Plain: Savannah River Site, South Carolina

John W. Shervais[1], Joshua Mauldin[1], Allen J. Dennis[2]

[1]Department of Geological Sciences
University of South Carolina
Columbia, SC

[2]Department of Biology and Geology
University of South Carolina-Aiken
Aiken, SC

Sumitted: December 1997
Revised: July 1998

Submitted To: Geological Society of America Special Paper:
Basement terranes of beneath the SE Atlantic Coastal Plain, Georgia and South Carolina: M.J. Bartholomew, editor.

Abstract: Over the last 35 years more than 5000 meters of basement core has been recovered from 26 deep wells at the Department of Energy's Savannah River Site. This core provides the only known exposure of basement terranes that lie SE of the Carolina terrane in central South Carolina, beneath Cretaceous and Tertiary sediments the Atlantic Coastal Plain. Core from six of these wells is dominated by metaplutonic rocks ranging from quartz diorite to granite in composition. Based on their modal and chemical compositions, metamorphic grade, and structural positions, basement cores are divided into two distinct units: the DRB Plutonic Suite (subcrop north of the Pen Branch Fault in core DRB-1), and the PBF Plutonic Suite (subcrop south of the Pen Branch fault in cores PBF-7, PBF-8, GCB-4, C-7, C-10, and SA).

Metaplutonic rocks of the DRB Plutonic Suite are represented by hornblende diorites, hornblende quartz diorites, and tonolites, which intrude metavolcanic wallrock. Metaplutonic rocks of the DRB Plutonic Suite display a wide compositional range, with SiO_2= 50-71%, MgO= 1.0-6.5%, K_2O ≤1%, TiO_2= 0.5-1.2%, and Fe_2O_3*= 2.9-12.2%, similar to the overall compositional range of the intruded metavolcanic wallrock. Rocks of the DRB Plutonic Suite were metamorphosed under upper greenschist to lower amphiblolite facies conditions. Metaplutonic rocks of the PBF Plutonic Suite were originally granodiorites with SiO_2= 55-72%, MgO < 5%, K_2O =1.4-3.2%, TiO_2= 0.5-1.7%, and Fe_2O_3*= 3.5-10%. Many metaplutonic rocks of the PBF Plutonic Suite have undergone extensive hydrothermal alteration, during which potassic fluids infiltrating along fractures replaced calcic feldspar with K-feldspar, causing severe depletion of CaO (0.5-2%) and Sr (≤160 ppm), adding K_2O (3.2-5.3%) and SiO_2 (72-77%), and coloring the rocks bright pink. Metamorphism of the PBF Plutonic Suite occurred primarily under upper amphibolite to lower granulite facies conditions, but the later hydrothermal alteration took place under greenschist facies conditions.

Metaplutonic rocks of both plutonic suites have calc-alkaline fractionation trends, consistent with formation in active, subduction-related arc terranes. Reported crystallization ages of ≈619 Ma to ≈626 Ma, however, show that these rocks do not correlate with accreted arc rocks in central South Carolina (Carolina slate belt, western Charlotte belt) because the latter are too young (≈535 to ≈570 Ma). Based on their compositions and ages, we tentatively correlate these rocks with the Hyco Formation in southern Virginia and central North Carolina. The Hyco Formation forms the infractructure of the Carolina terrane in Virginia and North Carolina, where it was affected by the circa 600 Ma "Virgilina" orogeny. The DRB/PBF arc may represent the infrastructure of the Carolina slate belt in South Carolina, detached by later tectonic events, or it may represent late Proterozoic arc infrastructure from another location in the arc that has been moved into its current location by transcurrent motions.

INTRODUCTION

The hinterland of the Southern Appalachians, which lies SE of Grenville basement exposed in the Blue Ridge province, comprises a complex mosaic of exotic terranes of uncertain provenance (e.g., Williams and Hatcher, 1982, 1983; Secor and others, 1983; Horton and others, 1989, 1991; Samson and others, 1990). These terranes include (from NW to SE) the Inner Piedmont, the Carolina terrane (including the Carolina slate belt), and the Raliegh belt (figure 1). Further to the SE, crystalline basement of the Laurentian margin is largely concealed beneath several kilometers of Mesozoic and Cenozoic sedimentary rocks, commonly referred to as the Atlantic Coastal Plain (Fallaw and Price, 1995; Colquhoun, 1991). This hidden crystalline basement is divided into additional terranes based on limited exposures at the margins of the Coastal Plain onlap, aeromagnetic lineaments that define basement trends in the subsurface, and core data from wells that penetrate basement (e.g., Horton and others, 1989, 1991).

The Savannah River Site and National Laboratory is located near the NW margin of the Atlantic Coastal Plain (figure 2), where up to 2 km of Cretaceous and younger sediments overlie crystalline rocks of the basement and a major Triassic rift basin (Dunbarton basin; Fallaw and Price, 1995; Cumbest and others, 1992, Snipes and others, 1993). Crystalline rocks of the Savannah River Site basement include mafic to felsic metavolcanic rocks, metagranitoids that intrude the metavolcanic rocks, and younger mafic and felsic dikes that cross-cut all older lithologies. These rocks are juxtaposed against high-grade metamorphic rocks of an unknown terrane to the north, and the Suwannee terrane (to the south) along major crustal discontinuities which can be mapped in the subsurface using magnetic and gravity potential field data. Although the Savannah River Site crystalline basement superficially resembles volcanic arc igneous suites of the Carolina terrane, it is separated from the greenschist facies rocks of the Carolina terrane, near Clarks Hill lake, by three separate fault zones. Understanding the development of this geologically complicated area requires careful characterization of the basement complex, and detailed comparisons with the rocks of adjacent terranes that may correlate with this basement complex.

In this report we present first a brief review of the regional geologic setting of the Savannah River Site, descriptions of the plutonic rock units sampled here, whole rock geochemical data on the plutonic igneous rocks, and finally, a discussion of how the crystalline basement rocks of the Savannah River Site formed and how they may correlate with other terranes exposed in the Piedmont of the Carolinas, Georgia, and Virginia.

REGIONAL SETTING

The SE margin of the Laurentian shield is generally defined by the eastern limit of the Blue Ridge province, a complex assemblage of older Grenville basement, metamorphosed continental margin sediments, intrusive rocks, and an accretionary complex (?) of metasediments, metabasalts, and ultramafic rocks (e.g., Bartholomew, 1984, and papers therein). Outboard of this province the Laurentian margin is plastered with a mosaic of "suspect" terranes that were accreted to the Laurentian margin during the Paleozoic, after Laurentia rifted from the western edge of Argentina and drifted north around the western margin of Gondwana (e.g., Dalziel and others, 1994). "Suspect" terranes that were accreted to the Laurentian margin during the Paleozoic include the Piedmont terrane (Inner Piedmont belt), the Carolina terrane (comprising the Kings Mountain belt, the Charlotte belt, and the Carolina slate belt), the Kiokee-Uchee-Dreher Shoals terrane, the Milledgeville terrane, and the Belair belt (Augusta terrane; figure 1). Each of these terranes contains different lithologic assemblages and have distinct geologic histories. Correlatations between these terranes is difficult because many formed as island arcs, and because age constraints are limited at this time. In this section we will review briefly the characteristics of these terranes; later we will discuss how these terranes may or may not correlate with crystalline basement of the Savannah River site.

Terranes NW of the Modoc Zone

Piedmont terrane: The Piedmont terrane consists of felsic to intermediate gneisses, migmatitic gneisses, and amphibolites exposed in northern Georgia, the western Piedmont of central South Carolina, and western North Carolina east of the Blue Ridge (figure 1). These rocks were metamorphosed to middle and upper amphibolite facies conditions and folded into a series of recumbent nappes (Griffin, 1971). Recently reported age determinations (Dennis and Wright, 1997a) suggest peak metamorphism ≈360 Ma, followed by retrograde overprinting ≈300 Ma during the Alleghanian orogeny.

Carolina terrane: The Carolina terrane consists of two distinct subunits: the amphibolite facies western Carolina terrane (Charlotte, Kings Mountain belts) and the greenschist facies eastern Carolina terrane (Carolina slate belt). The western Carolina terrane comprises mafic to intermediate metavolcanic rocks penetrated by a series of zoned, mafic-to-ultramafic intrusive complexes (Dennis and Shervais, 1991, 1996). Age determinations by Dennis and Wright (1997b) show that the zoned complexes crystallized and were deformed in the interval ≈575 Ma to 535 Ma. The metavolcanic rocks are commonly cross-cut by mafic dikes, including some containing abundant large pseudomorphs of actinolite after clinopyroxene. The protoliths of these pyroxene-megaphyric dikes were tholeiitic ankaramites that may represent the extrusive equivalent of the zoned mafic-

ultramafic complexes (Dennis and Shervais, 1991, 1996). These upper greenschist to lower amphibolite facies rocks are contiguous with somewhat higher grade rocks of the so-called *"Juliette terrane"* (Higgens and others, 1988), which forms the southwestern margin of the Carolina terrane (figure 1). Rocks of the Juliette terrane include felsic gneisses, amphibolites, and zoned mafic-ultramafic complexes — lithologies identical to those found in the Carolina terrane. Based on correlation of the Juliette terrane with the western Carolina terrane, we recommend that the term "Juliette terrane" be retired and that these rocks be included with the rest of the western Carolina terrane (e.g., Hooper and Hatcher, 1989; Dennis and Shervais, 1996).

The eastern Carolina terrane (Carolina slate belt) consists of greenschist facies felsic to intermediate tuffs, breccias, and flows, mudstones, and scarce mafic metavolcanics (Feiss, 1982; Rogers, 1982; Secor and others, 1982, 1986; Shelley, 1988; Shervais and others, 1996). Succession of the dominantly felsic metavolcanic rocks of the Persimmon Fork Formation by the mudstones and mafic metavolcanic rocks of the Richtex Formation (Secor and others, 1982, 1986) is interpreted to reflect evolution of the volcanic stratigraphy by intra-arc rifting (Dennis and Shervais, 1991, 1996; Shervais and others, 1996). The age of the eastern Carolina terrane is well constrained at ≈550 Ma by U-Pb zircon crystallization ages of shallow, epizonal granitic plutons that intrude the felsic metavolcanic rocks (Whitney and others, 1978; Carpenter and others, 1982; Dallmeyer and others, 1986; Barker and others, 1993). An upper age limit is constrained by a Middle Cambrian trilobite fauna found in the Asbill Pond Formation (Secor and others, 1983; Samson and others, 1990).

Where the Carolina terrane is exposed along the North Carolina-Virginia border, Glover and Sinha (1973) have shown that it was affected by folding and faulting ≈620-575 Ma during the Virgilina orogeny. Older rocks of the Carolina terrane in this area include the Hyco and Aaron formations, which are deformed and overlain unconformably by the Uwharrie Formation (≈Persimmon Fork Formation in central South Carolina). Most of the Carolina terrane in central South Carolina post-dates the Virgilina event (Dennis and Wright, 1997b).

Terranes SE of the Modoc Zone

The Carolina terrane is separated from a series of amphibolite facies subterranes to the SE by the Modoc zone, an early Alleghanian (≈310 Ma; Pray, 1997) normal fault (Snoke and others, 1980; Secor and others, 1986a; Sacks and Dennis, 1987). This complex fault system juxtaposes low-grade greenschist facies metavolcanic rocks of the Carolina slate belt against kyanite and sillimanite-grade rocks of the Uchee belt, Kiokee belt, and Dreher Shoals subterrane (figure 1). Snoke and Frost (1990) have shown that up to 25 km of structural deletion may have occured on the Modoc zone. Other terranes exposed SE of the Modoc zone include the lower grade

Milledgeville and Augusta terranes, and another, unnamed high-grade terrane exposed in a small window through sediments of the Coastal Plain (figure 2).

Kudzu terrane: The SE margin of the Modoc zone is bordered by high grade metamorphic rocks traditionally assigned to the Kiokee belt, Uchee belt, and Dreher Shoals subterrane. All three of these "terranes" are nearly identical lithologically, and had similar if not identical thermal histories. It seems likely that these "terranes" were originally one unit that was separated by later tectonic events or by coastal plain onlap. We propose here that these rocks be referred to as the **"Kudzu terrane"** (**K**iokee-**U**chee-**D**reher Shoals-Precambrian **Z**-**U**nified terrane).

Kiokee belt (aka "Savannah River terrane"): The Kiokee belt consists of upper amphibolite facies (sillimantite grade) migmatitic gneiss (biotite-amphibole paragneiss), sillimanite schist, amphibolite, luecocratic paragneiss, quartzite (chert?), and local ultramafic rocks (Maher, 1978, 1987; Maher and Sacks, 1987; Maher and others, 1991; Secor and others, 1986a, 1986b; Sacks and others, 1989). The predominance of migmatitic paragneiss and sillimanite schist indicates temperatures >650°C and minimum pressures ≥ 3 kb.

Uchee belt (aka "Uchee terrane"): The Uchee belt consists of upper amphibolite facies (sillimantite grade) migmatitic gneiss, schist, and amphibolite (Bentley and Neathery, 1970; Hanley, 1986; Chalokwu, 1989). Chalokwu (1989) determined a P-T range of ≈570-780°C at 7.0 to 9.2 kbars for amphibolites from this belt. It is nearly identical to the Kiokee belt lithologically.

Dreher Shoals "terrane": The Dreher Shoals terrane consists of upper amphibolite facies (staurolite-kyanite grade) schist, gneiss, amphibolite, and granitic orthogneiss (Secor and Snoke, 1978; Secor and others, 1986a; Dallmeyer and others, 1986; Snoke and Frost, 1990). Snoke and Frost (1990) determined a P-T range of ≈750°C at 7.2 t o 8.2 kbars — that is, nearly identical to the P-T ranges calculated by Chalokwu (1989) for the Uchee belt.

Milledgeville terrane: The Milledgeville terrane consists of upper greenschist to lower amphibolite facies mudstones, siltstones, and quartzites (metachert?), with local intercalations of metavolcanic rock (Pickering, 1976). Lithologically, it resembles rocks of the Richtex and Asbill Pond formations (Carolina slate belt). It may be fault bounded, or it may sit unconformably on top of the high-grade "Kudzu terrane".

Augusta terrane: The Augusta terrane (Maher and others, 1991), more commonly known as the Belair belt, is a small terrane exposed between the Kiokee belt and the onlap of the coastal plain (figure 2). The Augusta terrane consists of low-grade (greenschist facies) metavolcanic rocks and metasedimentary rocks with lithologic similarities to those of the Carolina terrane (Maher, 1978; Maher and others, 1991; Shervais and others, 1996). The metasedimentary rocks were originally

thin-bedded wackes and siltstones, interbedded with mafic to felsic crystal-lapilli tuff and, less commonly, amygdaloidal basalt (Shelley, 1988; Shervais and others, 1996). The only age constraint for rocks of the Augusta terrane is the presence of a lower Paleozoic trilobite segment (Maher and others, 1981).

The Augusta terrane is separated from the Kiokee belt by the Augusta fault, a late Alleghanian (≈275 Ma), low angle normal fault that has Augusta terrane rocks in its hanging wall (Maher, 1978, 1979; Maher and others, 1991). The Augusta terrane is separated from a higher grade terrane to the southeast by an aeromagnetic lineament (figure 2). This geophysically defined crustal block, which includes the Graniteville granite, appears to extend southward toward the Savannah River Site (figure 2).

Suwannee terrane: The Suwannee terrane, which underlies the coastal plain sediments of south Georgia, Alabama, and northern Florida, has only been sampled by drill core (Heatherington and Mueller, 1996; Heatherington and others, 1996; Mueller and others, 1994; Guthrie and Raymond, 1992). It consists of low-grade metavolcanic rocks (North Florida Volcanic Series) and intrusive rocks of diorite to granodioirite composition (the Osceola granite of central Florida and others). Reported zircon U-Pb ages include 552 Ma for a dacite metavolcanic of the North Florida Volcanic Series, 551 Ma for the Osceola granite, and 625 Ma for a granodiorite in southern Alabama (Heatherington and others, 1996; Mueller and others, 1994).

Whole rock geochemistry shows that the North Florida Volcanic Series and related intrusive rocks formed in a magmatic arc along the margin of Gondwana (Heatherington and Mueller, 1996; Heatherington and others, 1996; Mueller and others, 1994). Sr and Nd initial ratios indicate the involvment of both Proterozoic and Archean lithosphere. Metavolcanic and granitic rocks of the Suwannee terrane are age equivalent with the Carolina terrane, and may have formed in the same convergent margin setting.

Savannah River Site terrane: Major lithologic units of pre-Cretaceous basement beneath the Savannah River Site include the Crackerneck Metavolcanic Complex (subgreenschist facies metavolcanic rocks), the DRB Metavolcanic Complex (epidote-amphibolite facies metavolcanic rocks), the Pen Branch Metavolcanic Complex (amphibolite to lower granulite facies metavolcanic rocks), the PBF plutonic suite, the DRB plutonic suite, and clastic sedimentary rocks of the Triassic Dunbarton basin (figure 2). Metavolcanic rocks of the Crackerneck, DRB, and Pen Branch volcanic complexes are described in Mauldin et al. (this volume). The inferred occurrence of a Triassic-Jurassic mafic igneous complex south of the Dunbarton basin is based on aeromagnetic anomalies (Horton et al., 1991); core data from wells C-7 and C-10 indicate that much of this basement is "pinked" granite of the PBF plutonic suite. Younger, undeformed plutons

(the Devonian Springfield granite and the Carboniferous Graniteville granite) show that these rocks were last deformed prior to ≈400 Ma. The subsurface extent of these plutons is based on gravity anomalies, core data, and limited surface exposures (figure 2).

METHODS

Basement core was logged for 26 wells drilled in and around the Westinghouse/Savannah River Site, including wells drilled between ~1960 and 1994; the location of these wells and a geologic map based on subcrop lithology is shown in figure 4. Core from all wells studied here was logged for lithology and structural relationships, fractures, folds, foliations, layering, and relict primary intrusive contacts. Over 400 samples were collected, and from this collection 116 samples were selected for further petrologic study, including petrographic, mineral chemical, and/or whole rock geochemical analysis.

Quantitative electron microprobe analyses of major and minor elements were obtained with the Cameca SX50 four-wavelength-spectrometer automated electron microprobe at the University of South Carolina. The samples were examined optically and by secondary and backscattered electron imagery using the electron microprobe; analysis points were precisely located with a 1 μm precision sample stage. Analyses were made at 15 KV accelerating voltage, 30 nanoamperes probe current, and counting times of 20-40 seconds, using natural and synthetic mineral standards. Analyses were corrected for instrumental drift and deadtime, and electron beam/matrix effects using the "PAP" $\phi(\rho z)$ correction procedures provided with the Cameca microprobe automation system; these correction procedures are based on the model of Pouchou and Pichoir (1991). Analytical precision is ≈1% of the amount present for oxide concentrations greater than 10 wt%, 1-2% for oxide concentrations between 1 and 10 wt%, and 5-10% for oxide concentrations between 0.01 and 1 wt%. Relative accuracy of the analyses, based upon comparison of measured and published compositions of the standards, is ~1-2% for oxide concentrations greater than 1 wt% and ~10% for oxide concentrations less than 1 wt%. Mineral analyses are presented in Table 1.

Thirty-five plutonic rocks were selected for whole rock major and trace element geochemistry. Each sample was analyzed for 10 major elements (SiO_2, TiO_2, Al_2O_3, total Fe as Fe_2O_3*, MnO, MgO, CaO, Na_2O, K_2O, P_2O_5) and 12 trace elements (Nb, Zr, Y, Sr, Rb, Zn, Cu, Ni, Cr, Sc, V, Ba) using the University of South Carolina's Philips PW-1400 X-ray fluorescence spectrometer. Major elements were analyzed on fused glass disks using a method similar to Taggart and others (1987); trace elements were analyzed using pressed powder briquettes prepared using the technique of Holland and Brindle (1966). Calibration curves and matrix corrections were established using a series of selected USGS and international standards (Potts and others, 1992) and the Philips X41 software package. Replicate analyses of selected standards as unknowns show percent relative

errors of ≈1% for silica, ≈2-4% for less abundant major elements, and ≈6-7% for elements with concentrations < 0.5 wt%. Eleven whole rock samples were also analyzed for rare earth element (REE) concentrations by inductively coupled argon plasma/mass spectrometry (ICP-MS) at the University of New Mexico.

DESCRIPTION OF METAPLUTONIC UNITS BENEATH THE SAVANNAH RIVER SITE

The DRB Plutonic Suite

The DRB Plutonic Suite is sampled exclusively by the 4" diameter Deep Rock Borehole (DRB) core DRB-1 (Mauldin and others, 1997; Roden and others, 1997). It consists dominantly of diorite and quartz diorite sheets that intrude preexisting metavolcanic wallrock; both are cut by younger mafic dikes. The DRB metadiorites were metamorphosed to epidote-amphibolite facies assemblages, and range texturally from equigranular to porphyritic gneisses. The porphyritic gneisses are characterized by large, zoned hornblende and plagioclase porphyroclasts, within a fine to medium-grain matrix of plagioclase, quartz, chlorite, blue/green amphibole, and epidote (figure 3). Chloritic fractures and chloritized amphiboles may also appear sparsely.

Most amphibole porphyroclasts, and essentially all groundmass amphiboles, are metamorphosed to blue-green amphibole. However, many amphibole porphyroclasts preserve cores of brown hornblende, which are interpreted to represent relict igneous hornblende (figure 3a). Relict igneous hornblende is characterized by higher Mg/Fe ratios (figure 4a), higher Al_2O_3, and higher TiO_2 than the metamorphic blue-green amphibole. These differences are shown clearly in a plot of tetrahedral Al vs Ti, where metamorphic amphibole has $Al^{IV} > 1.4$ afu (atomic formula units per 23 oxygen) and Ti < 0.06 afu (figure 5). Coexisting igneous hornblende has higher Ti (0.03 to 0.45 afu, with most > 0.1 afu Ti) and lower Al^{IV} (< 1.35 afu; figure 5).

Less commonly, the blue-green metamorphic amphiboles contain cores of fibrous actinolite defining large sub- to anhedral porphyroclasts. Actinolite is characterized by low Al^{IV} (~0.4 afu; figure 5). These actinolite cores may represent pseudomorphs after primary igneous hornblende, or possibly even pyroxene, that was retrograded to actinolite under later greenschist facies conditions. The textural relations are interpreted to indicate that the greenschist facies minerals (actinolite, chlorite) post-date the amphibolite facies assemblage and must represent retrograde metamorphism, not an older phase of seafloor metamorphism that pre-dates higher grade metamorphism (e.g., Roden and others, 1997).

Plagioclase porphyroclasts may show relict igneous features, including oscillatory zoning and albite twinning (figure 3b). Average plagioclase compositions usually fall between An_{15} and An_{30}

(figure 6). However, individual porphyroclasts may have cores as calcic as An_{40} and rims as sodic as An_9 (figure 6a; Table 1). The calcic cores are interpreted to represent relict igneous plagioclase compositions; the sodic rims formed during metamorphism along with the blue-green amphibole (e.g., Roden and others, 1997). Metaplutonic rocks of DRB-1 contain no garnet, consistent with metamorphism at relatively low temperatures and pressures (lower amphibolite to uppermost greenschist facies conditions). Biotite is rare to absent in the DRB metadiorites; almost all primary biotite has been metamorphosed to chlorite.

A number of mylonite zones penetrate the DRB-1 metadiorites. These may be distinguished by belts of ultrafine-grained quartz, feldspar, amphibole, and epidote bounded on either side by fine to medium grained porphyritic gneisses. The mylonite zones are generally meter scale in thickness.

PBF Plutonic Suite

The PBF Plutonic Suite forms a thin slice of crystalline basement between the Triassic Dunbarton basin to the south and the more extensive DRB Metavolcanic Complex to the north (figure 2). The PBF Plutonic Suite dominates the upper part of the core recovered from wells PBF-7, PBF-8, C-10, GCB-4, and the Seismic Attenuation well (SA); metavolcanic rocks of the Pen Branch Volcanic Complex are found in the deeper core from these wells. The PBF Plutonic Suite comprises two dominant lithologies: gneissic metagranitoids and "pinked" metagranitoids, formed by hydrothermal alteration of the normal gneissic metagranitoids (Mauldin and others, 1997; Dennis and others, this volume).

Gneissic Metagranitoids: "Unpinked" gneissic metagranitoids of the PBF Plutonic Suite are porphyroclastic gneisses with porphyroclasts of amphibole and plagioclase set in a groundmass of amphibole, plagioclase, microcline, biotite, quartz, and epidote (figure 7a). Amphibole porphyroclasts are unzoned and similar in appearance to the blue-green amphiboles found in the DRB metadiorites (figure 7b). Amphiboles have Mg/Fe ratios similar to the metamorphic amphiboles in the DRB metadiorites (figure 4b), but TiO_2 values range from 0.7% to 1.0%, higher than metamorphic amphibole in the DRB metadiorites. Blue-green amphibole in the PBF metaplutonic rocks is clearly distinguished from the relict igneous hornblende of the DRB Plutonic Suite, however, by its higher Al^{IV} (> 1.42 afu; figure 5). Plagioclase porphyroclasts within the PBF gneisses range from An_{24} to An_{38} and have an average composition of An_{35} (figure 6b).

Despite their superficial similarity to metadiorites of the DRB Plutonic Suite, the PBF gneissic metagranitoids are distinguished by their lack of relict igneous hornblende, the relatively high Ti in blue-green metamorphic amphibole, higher An-content plagioclase, the common occurrence of microcline, and the preservation of biotite. Some of these characteristics may result from higher

metamorphic grade in the PBF metagranitoids, but others (e.g., common microcline) reflect fundamental compositional differences between the two intrusive series.

Pinked metagranitoid: Much of the granitic core recovered from wells PBF-7, PBF-8, C-10, and SA was subjected to partial to extensive hydrothermal alteration that post-dates formation of foliation. We refer to this alteration as the "pinking" event due to the salmon-pink color imparted upon rocks affected by the hydrothermal fluids. The effects of this "pinking" event range from mm-scale selvages on fractures to pervasive alteration of hundreds of meters of core (Dennis and others, this volume).

"Pinked" PBF metagranites commonly contain large plagioclase, microcline, and garnet porphyroblasts set in a finer-grained matrix of quartz, plagioclase, microcline, and chlorite. Plagioclase porphyroblasts are much less common in pinked rocks. Amphibole is almost completely chloritized, but some relict blue-green amphibole is preserved. Microcline in the pinked metagranitoids commonly occurs as large megacrysts up to ~5mm across, and may account for as much as 40% of the modal mineralogy. Partially pinked rocks have plagioclase An_{25} to An_{33} (figure 6b). Plagioclase in the thoroughly pinked granites is completely albitized (An_4), and subsequently, partially sericitized (figure 6b). Biotite, like amphibole, also has been almost completely chloritized.

WHOLE ROCK GEOCHEMISTRY

Whole rock geochemical data by x-ray fluorescence analysis for 35 samples of plutonic rock are presented in Table 2; REE analyses of 11 samples by ICP-MS are presented in Table 3. All of the samples are metamorphosed but because these samples were recovered by deep coring of the basement, none was subjected to subaerial weathering.

DRB Plutonic Suite

Metaplutonic rocks sampled by core from DRB-1 may be classified as diorites or quartz diorites based on their normative mineralogy (figure 8). Whole rock geochemical data for the DRB-1 metadiorites show major and trace element trends typical of calc-alkaline intrusive suites: MgO, Fe_2O_3*, TiO_2, CaO, Al_2O_3, Sr, Cr, and Ni all decrease with increasing SiO_2, whereas Na_2O, K_2O, and Rb all increase (figure 9). At any given silica mode, the DRB metadiorites are lower in mafic elements (Mg, Fe, Ti, Cr, Ni), K_2O, and Rb than the PBF metagranitoids described below, and higher in plagiophile elements (Ca, Na, Al). The DRB metadiorites are calc-alkaline on an AFM plot (figure 10), consistent with their observed lack of Fe or Ti enrichment on Harker diagrams.

Four samples were chosen for REE analysis (Table 3). All are enriched in the light rare earth elements (LREE) relative to the heavy rare earth elements (HREE), with La ≈10x–30x chondrite,

and La/Lu ratios of ≈2.3x–3.8x chondrite (figure 11). The La/Lu ratios are lower than those observed in rocks of the DRB Metavolcanic Complex (Mauldin and others, this volume). All four samples have small negative Eu anomalies, which imply that plagioclase fractionation played a role in the petrogenesis of these rocks.

PBF Plutonic Suite

Metagranitoids: Gneissic metagranitoids sampled by core from PBF-7, PBF-8, C10, GCB-4, and the Seismic Attenuation well (SA) may be classified as "quartz monzodiorites" and "granodiorites" using their normative mineralogy (figure 8). Whole rock geochemical data for the PBF metagranitoids show major element trends similar to those of DRB-1: MgO, Fe_2O_3*, TiO_2, CaO, Al_2O_3, Sr, Cr, and Ni all decrease with increasing SiO_2, whereas Na_2O, K_2O, and Rb all increase (figure 9). At any given silica mode, the PBF metagranitoids are higher in mafic elements (Mg, Fe, Ti, Cr, Ni), K_2O, and Rb than the metadiorites of DRB-1, and lower in plagiophile elements (Ca, Na, Al). Like the DRB-1 diorites, the PBF metagranitoids are strongly calc-alkaline on an AFM plot (figure 10).

Six "unpinked" metagranitoids of the PBF intrusive complex were analyzed for REE concentrations (Table 3). All are enriched in LREE relative to HREE, with La ≈30x–100x chondrite, and La/Lu ratios of ≈3.6x to ≈5.4x chondrite (figure 11). Both the La/Lu ratios and total REE are higher than those observed in metadiorites of the DRB plutonic suite. Five of these samples have small negative Eu anomalies, suggesting plagioclase fractionation, whereas one has a significant positive Eu anomaly, suggesting plagioclase accumulation (figure 11).

Pinked metagranitoids: Almost all of the metagranitoids in the PBF-7 core between ~950m to ~1100m below the surface (footage 3100' to 3600') were partially to completely altered by a greenschist facies hydrothermal event that increased the modal K-feldspar content, albitized plagioclase, and altered biotite and hornblende to chlorite (see description of the lithologic units, above). The most striking physical feature of these altered rocks is their bright salmon-pink color, which may form selvages on fractures in partially altered rocks, or completely color the rock in more intensely altered horizons. Similar pink granitoids are found in other deep cores from the PBF formation (PBF-8, SA, C10).

Metagranitoid samples that were thoroughly "pinked" are characterized by higher SiO_2, K_2O, and Rb than their unaltered equivalents, and by lower MgO, Fe_2O_3*, TiO_2, Al_2O_3, CaO, Na_2O, and Sr (figure 9). As a result, these rocks are classified as "granites" using their normative mineralogy (figures 8). They extend the strong calc-alkaline trend of the "unpinked" metagranitoids (figures 9 and 10), but this apparent calc-alkaline "fractionation trend" results from hydrothermal alteration, not igneous processes.

Only one sample of "pinked" PBF-7 was analyzed for REE concentrations (PBF-7-3568). This sample is characterized by modest LREE enrichment (La/Lu ~2.1x chondrite) and by a pronounced negative Eu anomaly not seen in the "unpinked" PBF-7 metagranitoids (figure 11). This suggests that Eu^{2+} (and possibly other LREE) was mobilized along with Ca^{2+} during the "pinking event" and removed from the system.

DISCUSSION

Metaplutonic rocks of the DRB and PBF plutonic suites exhibit compositional ranges and phase assemblages consistent with formation in subduction-related volcanic arcs. Deciphering the nature of these arcs requires consideration of the magmatic evolution of each complex, its age and isotopic composition, its trace element characteristics, and its subsequent metamorphic history.

Fractionation Modeling: The smooth compositional trends exhibited by these rocks on Harker diagrams suggest fractional crystallization as the dominant process controlling composition (figure 9). Other processes which could have played an important role in the petrogenesis of these rocks are magma mixing and assimilation. In order to evaluate fractional crystallization as the controlling process, we chose three relatively primitive compositions from our analyzed dataset as potential "parent magmas" and modeled their fractionation paths using the computer program COMAGMAT (Ariskin and others, 1993). The three samples chosen as potential parent magmas are DRB-1-1438 (an older amphibolite dike), DRB-1-1047 (the most primitive diorite), and DRB-4-1758 (a mafic metavolcanic rock). Fractionation trends were calculated for two different sets of conditions: (1) QFM oxygen buffer, 2 kb total pressure, pyroxene = pigeonite, no water and (2) NNO+1.0 oxygen buffer, 3 kb total pressure, pyroxene = opx, and 1% water. The different conditions seem to have only a minor effect on calculated fractionation trends, which depend mostly on the starting magma composition (figure 9). These models are limited by the inability of the program to model hornblende fractionation directly, especially since hornblende is the most prominent mafic igneous phase.

In general, the calculated fractionation trends provide good matches to the observed range in data, with some suggestion that more than one parent magma is required to explain the observed compositions. Only a few samples have compatible element concentrations (Cr, Ni) that plot above calculated fractionation trends, which suggests that magma mixing between evolved melts and influxes of primitive magma was not an important process in these rocks. The incompatible elements K and Rb have observed concentrations that plot above calculated fractionation trends, but only for PBF granitoids and "pinked" granites (figure 9). This is consistent with post-crystallization enrichment in these elements during the "pinking" event, as discussed earlier. In

addition, the parent magma compositions used in the models may not be appropriate for the PBF series granitoids.

Age Constraints and Tracer Isotopes: Two samples were dated using the U-Pb zircon method (Dennis and others, 1997). Quartz monzodiorite from PBF-7 is slightly older at 626.1±4.4 Ma; DRB-1 quartz diorite is 619.2±3.4 Ma (Dennis and others, 1997). These late Proterozoic ages are too old to correlate with the Carolina slate belt (≈550 Ma; Whitney and others, 1978; Carpenter and others, 1982; Dallmeyer and others, 1986; Barker and others, 1993) or the western Carolina terrane (≈535 Ma to 580 Ma; Dennis and Wright, 1997b), but similar ages have been determined for the Hyco Formation in central North Carolina (Harris and Glover, 1988). The Hyco Formation represents the infrastructure of the Slate Belt arc in North Carolina and Virginia, where it is overlain unconformably by the Uwharrie formation (=Persimmon Fork Formation of the Carolina Slate Belt in South Carolina).

Tracer isotopes indicate derivation of both the DRB diorites and PBF granodiorites from similar, relatively primitive sources. The DRB-1 diorite has a calculated initial $^{87}Sr/^{86}Sr$ ratio of 0.70194 and ε_{Nd}+3.5; PBF granodiorite has a calculated initial $^{87}Sr/^{86}Sr$ ratio of 0.70318 and ε_{Nd}+2.0 (Dennis and others, 1997). The PBF-7 initial Sr ratio was calculated in two steps to correct for the effects of "pinking" on the measured Rb concentration. These values of initial Sr and ε_{Nd} are similar to those that have been measured on meta-igneous rocks of the Carolina terrane and other peri-Gondwana "Avalonian" terranes (e.g., Nance and others, 1991; Nance and Murphy, 1996).

Metamorphism: Meta-igneous rocks of both the DRB and PBF plutonic suites preserve evidence for similar metamorphic histories. These histories are best illustrated by the changes in amphibole composition (figure 5). Relict igneous hornblende compositions are preserved in the cores the larger plutonic amphiboles. These compositions are overprinted by the pervasive growth of blue-green metamorphic amphibole, consistent with amphibolite facies metamorphism. The high temperature blue-green amphiboles were susequently retrograded to the greenschist facies minerals actinolite and chlorite. Garnet-biotite geothermometry of metavolcanic rocks associated with the plutonic rocks in core suggest equilibration temperatures of ≈650°C for the DRB Metavolcanic Complex (amphibolite facies), and ≈700°C to ≈840°C for the Pen Branch Metavolcanic Complex (upper amphibolite to granulite facies; Mauldin and others, this volume).

Hydrothermal Alteration: The Big Pink: Many metaplutonic rocks of the PBF formation were affected by a post-metamorphic hydrothermal alteration event whose characteristic signature is a pervasive discoloration of the normally gray rocks to various shades of bright salmon-pink. The metamorphic phase assemblage associated with this event (actinolite, chlorite, albite, K-feldspar)

indicates greenschist facies metamorphism at temperatures ≈350°C to ≈450°C. The primary geochemical characteristic of this event is Si, K, and Rb metasomatism of the affected rocks by hydrothermal fluids, and concommitant leaching of Ca and Eu^{2+}. We suggest that the breakdown of primary biotite to chlorite, which is nearly complete in the pinked samples and affects much of the DRB plutonic suite, is the most likely source of these alkalis.

Data presented by Dennis and others (this volume) and by Heath and Bartholomew (this volume) show that the "pinking" event pre-dates the formation of most filled-fractures. The best estimate for the absolute age of this event is the Rb-Sr "isochron" presented by Kish (1992) for granite from core C10. This two point pseudo-isochron, based on the whole rock and a K-feldspar separate, must represent the age of the "pinking" event because the pervasive K and Rb metasomatism of this event would thoroughly reset the isotopic systematics of the K-feldspar, which controls the slope of the isochron. The "isochron" yields a model age of ≈220 Ma (early Triassic), which implies that the "pinking" event was associated with early Mesozoic rifting of North America from NW Africa, and the formation of the Dunbarton basin. This is consistent with the conclusions of Heath and Bartholomew (this volume), based on fracture relations observed in quarries.

Origin of the DRB/PBF Volcanic Arcs: Despite their gross similarity, plutonic rocks of the DRB and PBF plutonic suites exhibit significant differences which lead us to conclude that they do not represent the same rock series, although they may be related. Major differences include:

1. The DRB plutonic suite is dominated by quartz diorite, the PBF plutonic suite is dominated by quartz monzodiorite (unpinked) and granite (pinked).

2. Diorites of the DRB plutonic suite and quartz monzodiorites of the PBF plutonic suite have distinct, subparallel trends on Harker diagrams that are offset from one another. At any given silica content, the DRB metadiorites are lower in mafic elements (Mg, Fe, Ti, Cr, Ni), K_2O, and Rb than PBF metagranitoids, and higher in plagiophile elements (Ca, Na, Al). These differences must reflect different parent magmas and different magma source regions.

3. Diorites of the DRB plutonic suite have lower REE concentrations, and lower La/Lu ratios than plutonic rocks of the PBF plutonic suite. These differences are too large to result from fractionation processes, and must reflect different parent magmas and different magma source regions.

4. Diorite of the DRB plutonic suite has lower initial $^{87}Sr/^{86}Sr$ (0.70194) and higher ε_{Nd} (+3.5) than PBF granodiorite (initial $^{87}Sr/^{86}Sr = 0.70318$, ε_{Nd}+2.0). These data indicate an oceanic affinity for the DRB intrusive complex, and a weak continental influence on the PBF intrusive complex.

5. Rocks of the PBF plutonic suite were metamorphosed to higher grades than those of the DRB plutonic suite (upper amphibolite to granulite facies *versus* lower to middle amphibolite facies). The higher grade of the PBF plutonic suite indicates equilibration at deeper crustal levels relative to the DRB plutonic suite.

The evidence listed above shows that metaplutonic rocks of the DRB and PBF plutonic suites are not equivalent, and must represent different magmatic systems. They may have formed within the same arc in different places, or at different times; alternately, they may also have formed in unrelated arc terranes and only been juxtaposed later. Their closely similar ages and isotopic compositions argue against both of the latter hypotheses, and strongly suggest that they formed within the same arc system, in somewhat different places.

The lack of Fe and Ti enrichment, the range in SiO_2 contents, and the calc-alkaline trends on AFM diagrams all suggest that both the DRB and the PBF plutonic suites represent relatively mature arcs. Diorites of the DRB plutonic suite are confined to relatively primitive compositions, and do not exhibit the more extended compositional range seen in the DRB Metavolcanic complex (Mauldin and others, this volume). The low normative quartz contents, relatively primitive major element compositions, low total REE, low La/Lu, low initial $^{87}Sr/^{86}Sr$, and high ε_{Nd} of the DRB diorites are interpreted to indicate that this plutonic suite formed in a magmatic arc that was built on older oceanic or arc crust, and that continental crust was not part of its autochonous basement.

In contrast, quartz monzodiorites of the PBF plutonic suite are more potassic than the DRB diorites, and are enriched in mafic elements (at similar silica modes), have higher total REE, higher La/Lu, higher initial $^{87}Sr/^{86}Sr$, and high ε_{Nd}. This suggests derivation from a more evolved source, such as an older, more mature oceanic arc terrane or a continental margin arc built on "transitional" crust. These differences may be analogous to the "quartz diorite line" in the western Sierra Nevada arc, which separates arc plutons intruded through accreted oceanic or arc-derived crust on one side (quartz diorites) from arc plutons intruded through older cratonic crust on the other side (granites, granodiorites).

Correlation of the DRB and PBF Plutonic Suites: The data presented here show that metaplutonic rocks of the DRB and PBF plutonic suites formed in subduction-related volcanic arcs during the

late Proterozoic, ≈620-625 Ma. They share similar Sr and Nd isotopic systematics, which are also similar to other peri-Gondwana arc terranes (e.g., Nance and others, 1991; Nance and Murphy, 1996). The closely similar ages and isotopic compositions argue against formation in different arcs or at different times in the same arc. The DRB/PBF arc cannot be correlated with the proximal Carolina slate belt (Persimmon Fork Formation) in central South Carolina because (a) the Persimmon Fork Formation is too young at ≈550 Ma, and (b) the Persimmon Fork formation is dominated by felsic to intermediate composition volcanic rocks, not the basalt to dacite volcanic rocks that dominate the DRB/PBF arc. The DRB/PBF volcanic arc is also older than the western Carolina terrane (e.g., Dennis and Wright, 1997b), although the DRB/PBF metagranitoids are lithologically similar to rocks of the western Carolina terrane.

The DRB/PBF volcanic arc may correlate with the Hyco Formation in central North Carolina and southern Virginia (Harris and Glover, 1988). The Hyco Formation consists of mafic to felsic metavolcanic rocks dated at ≈620 Ma (Glover and Sinha, 1973). These rocks were deformed and metamorphosed during the ≈600 Ma "Virgilina orogeny" of Glover and Sinha (1973), and then overlain unconformably by younger arc rocks of the Uwharrie Formation and Albemarle Group (Harris and Glover, 1988). The Uwharrie Formation was affected by minor deformation and low-grade metamorphism, but lacks fabric elements of the older Virgilina event.

The Uwharrie Formation correlates with the Persimmon Fork Formation of central South Carolina both lithologically and in age. Thus, one possible interpretation of the DRB/PBF volcanic arc is that it represents infrastructure of the Carolina terrane in South Carolina that was detached by later tectonic events. Alternatively, it may represent late Proterozoic arc infrastructure from another location in the arc, that was moved into its current location by transcurrent motions.

Acknowledgements: The authors wish to thank Randy Cumbest and Sharon Lewis of Westinghouse/SRC for their moral and logistical support, and Westinghouse/SRC for access to their core storage facility. Sample preparation for XRF analyses was carried out by Hampton Grove, Morris Minor, and Neal Wicker. Scott Vetter of Centenary College and Chip Shearer of the University of New Mexico provided the ICP-MS analyses. This work was funded by the U.S. Department of Energy through Westinghouse/SRC, SCUREF Task 170.

REFERENCES CITED

Ariskin, AA, Frenkel, MY, Barmina, GS, Nielsen, RL, 1993, Comagmat: A Fortran program to model magma differentiation processes. Computers and Geosciences, Vol 19, No 8, pp 1155-1170.

Barker, C.A., Secor, D.T., Pray, J.R., Dallmeyer, R.D., Jr., and Wright, J.E., 1993, Tectonothermal history of the Carolina terrane: evidence for late Proterozoic deformation in northeast South Carolina, *South Carolina Academy of Sciences Bulletin*, **55**, 63.

Bentley, R. D., and Neathery, T. L., 1970, Geology of the Brevard fault zone and related rocks of the Inner Piedmont of Alabama, *in* Bentley, R. D., and Neathery, T. L., eds., Geology of the Brevard fault zone and related rocks of the Inner Piedmont of Alabama: Alabama Geological Society, 8th Annual Field Trip Guidebook, 1-79.

Carpenter, R. H., Odom, A. L., and Hartley, M. E., III, 1982, Geochronological investigation of the Lincolnton metadacite, Georgia and South Carolina, *in* Bearce, D. N., Black, W. W., Kish, S. A., and Tull, J. F., eds. Tectonic studies in the Talladega and Carolina slate belts, southern Appalachian orogen: *Geological Society of America, Special Paper 191*, 145-152.

Chalokwu, C. I., 1989, Epidote-amphibolite to amphibolite facies transition in the southern Appalachian Piedmont: P-T conditions across the garnet and calc-silicate isograds: *Geology*, **17**, 491-494.

Colquhoun, D.J., 1991, Southeastern Atlantic regional cross-section, eastern and offshore, South Carolina and Georgia sectors, American Association of Petroleum Geologists.

Cumbest, R.J., Price, Van, and Anderson, Eric E. (1992) Gravity and magnetic modeling of the Dunbarton Triassic basin, South Carolina, Southeastern Geology, 33, 37-51.

Dallmeyer, R. D., Wright, J. E., Secor, D. T., Jr., and Snoke, A. W., 1986, Character of the Alleghanian orogeny in the southern Appalachians: Part II. Geochronological constraints on the tectonothermal evolution of the eastern Piedmont in South Carolina: *Geological Society of America Bulletin*, **97**, 1329-1344.

Dalziel, I.W.D., Dalla Salda,, L.H., and Gahagan, L.M., 1994, Paleozoic Laurentia-Gondwana interaction and the origin of the Appalachian-Andean mountain system, Geological Society of America Bulletin, 106, 243-252.

Dennis, A.J. and Shervais, J.W., 1991, Arc rifting of the Carolina terrane in northwestern South Carolina. *Geology*, **19**, 226-229.

Dennis and Shervais, J.W., 1996, The Carolina terrane in northwestern South Carolina: Insights into the development of an evolving island arc; in "*Avalonian and Related Terranes of the Circum-Atlantic*, D. Nance (ed), Geol. Soc. America Special Publication 304, 237-256.

Dennis, A. J., and Wright, J. E., 1993, New late Precambrian-Cambrian U-Pb zircon ages for zoned intrusives in the western Carolina terrane, Spartanburg and Union Counties, South Carolina: *Geological Society of America Abstracts with Programs,* **25,** A12.

Dennis, A. J., and Wright, J. E., 1995, Mississippian (ca. 326-323 Ma) U-Pb crystallization ages for two granitoids in Spartanburg and Union Counties, South Carolina, *in* Dennis, A. J., Butler, J. R., Garihan, J. M., Ranson, W. A., and Sargent, K. A., eds., Geology of the western part of the Carolina terrane in northwestern South Carolina: Columbia, South Carolina Geological Survey, Carolina Geological Society Field Trip Guidebook for 1995, South Carolina Geology, **37**, 23-28.

Dennis and Wright, J.E., 1997a, Middle and late Paleozoic monazite U-Pb ages, Inner Piedmont, South Carolina, *Geological Society of America Abstracts with Programs,* **29/3,** 12.

Dennis, A. J., and Wright, J. E., 1997b, The Carolina terrane in northwestern South Carolina, USA: Late precambrian-Cambrian deformation and metamorphism in a peri-Gondwana oceanic arc: *Tectonics*, **16**, 460-473.

Dennis, A. J., Sacks, P. E. & Maher, H. D. 1987. Nature of the late Alleghanian strike- slip deformation in the eastern South Carolina Piedmont: The Irmo shear zone. In: *Anatomy of the Alleghanian orogeny as seen from the Piedmont of South Carolina and Georgia* (edited by Secor, D. T., Jr.). Columbia, South Carolina Geological Survey, Carolina Geological Society Field Trip Guidebook for 1987, 49-66.

Dennis, A.J., Wright, J.E., Maher, H.D., Mauldin, J.C., and Shervais, J.W., 1997, Repeated Phanerozoic reactivation of a southern Appalachian fault zone beneath the updip coastal plain of South Carolina, *Geol. Soc. America, Abstracts w/Programs*, Salt Lake City, **29/5**, A12.

Dennis, A.J., Maher, H.D., Mauldin, J.C., and Shervais, J.W. (this volume) Repeated Phanerozoic reactivation of a southern Appalachian fault zone beneath the Savannah River Site, South Carolina, *in* Bartholomew, M.J. (ed) *Basement terranes of beneath the SE Atlantic Coastal Plain, Georgia and South Carolina*: Geological Society of America Special Paper, in press.

Fallaw, W.C. and Price, Van (1995) Stratigraphy of the Savannah River site and vicinity, *Southeastern Geology*, 35, 21-58.

Feiss, P. G., 1982, Geochemistry and tectonic setting of the volcanics of the Carolina slate belt: *Economic Geology*,, **77**, 273-293.

Glover, L., III, and Sinha, A. K., 1973, The Virgilina deformation, a late Precambrian to Early Cambrian (?) orogenic event in the central Piedmont of Virginia and North Carolina: *American Journal of Science*, **273-A**, 234-251.

Griffin, V., 1971, Inner Piedmont belt of the southern crystalline Appalachians,Geological Society of America Bulletin, 82, 1885-1898.

Guthrie and Raymond, 1992, Pre-middle Jurassic rocks beneath the Alabama Gulf Coastal Plain; Alabama Geological Survey Bulletin 150, 68 pp.

Hanley, T. B., 1986, Petrography and structural geology of Uchee belt rocks in Columbus, Georgia, and Phenix City, Alabama, *in* Neathery, T. L., ed., Southeastern Section of the Geological Society of America: Boulder, Colorado, Geological Society of America Centennial Field Guide, **6**, 297-300.

Harris, C. W., and Glover, L., III, 1988, The regional extent of the ca. 600 Ma Virgilina deformation: Implications for stratigraphic correlation in the Carolina terrane: *Geological Society of America Bulletin*, **100**, 200-217.

Heath, R.D. and Bartholomew, M.J., this volume, Mesozoic phase of post-Alleghanian deformation in the Appalachian piedmont, *in* Bartholomew, M.J. (ed) *Basement terranes of beneath the SE Atlantic Coastal Plain, Georgia and South Carolina*: Geological Society of America Special Paper, in press.

Heatherington, A.L., Mueller, P.A., Nutman, A.P., 1996, Neoproterozoic magmatism in the Suwannee terrane: Implications for terrane correlations, *in* Nance, R. D., and Thompson, M., eds., Avalonian and related peri-Gondwanan terranes of the circum-North Atlantic: *Geological Society of America Special Paper 304*, 219-236.

Heatherington, A.L., Mueller, P.A., 1996, Geochemistry and origin of Floridan crustal basement terranes, *in* Randazzo, A. and Jones, D., eds., Geology of Florida; Gainesville, University of Florida Press.

Higgins, M. W., Atkins, R. L., Crawford, T. J., Crawford, R. F., III, Brooks, R., and Cook, R. B., 1988, The structure, stratigraphy, tectonostratigraphy, and evolution of the southernmost part of the Appalachian orogen: U. S. Geological Survey Professional Paper 1475, 173 p.

Holland, T. and Blundy, J., 1994, Non-ideal interactions in calcic amphiboles and their bearing on amphibole-plagioclase thermometry, Cont. Mineral. Petrol., 116, 433-447.

Holland and Brindle, 1966, *Spectrochimica Acta*, **23**, 2083-2093.

Hooper, R. J., and Hatcher, R. D., Jr., 1989, The geology of the east end of the Pine Mountain window and adjacent Piedmont, central Georgia: Atlanta, Georgia, Georgia Geological Society, Premeeting Field Trip Guide for the 1989 Southeastern Section Meeting, Geological Society of America, 37 p.

Horton, J. W., Jr. Drake, A. A., Jr. and Rankin, D. W., 1989, Tectonostratigraphic terranes and their Paleozoic boundaries in the central and southern Appalachians, *in* Dallmeyer, R. D., ed. Terranes in the circum-Atlantic Paleozoic Orogens: *Geological Society of America Special Paper 230*, 213-245.

Horton, J. W., Jr., Drake, A. A., Jr. Rankin, D. W., and Dallmeyer, R. D., 1991, Preliminary tectonostratigraphic terrane map of the central and southern Appalachians: U. S. Geological Survey Miscellaneous Investigations Series Map I-2163, scale 1:2,000,000, 1 sheet.

Jones, L. M., and Walker, R. L., 1973, Rb-Sr whole-rock age of the Siloam granite, Georgia: A Permian intrusive in the southern Appalachians: *Geological Society of America Bulletin*, **84**, 3653-3657.

Kish, S.A., 1992, An initial geochemical and isotopic study of granite from core C-10, Savannah River Site, South Carolina, *in* W. Fallaw and V. Price, eds., *Geological Investigations of the Central Savannah River Area, South Carolina and Georgia*, Carolina Geological Society Field Trip Guide Book.

Maher, H. D., 1978, Stratigraphy and structure of the Belair and Kiokee belts, near Augusta, Georgia, *in* Snoke, A. W., ed., Geological investigations of the eastern Piedmont, southern Appalachians: Columbia, South Carolina Geological Survey, Carolina Geological Society Field Trip Guidebook for 1978, 47-54.

Maher, H. D., 1979, Stratigraphy, metamorphism, and structure of the Kiokee and Belair belts near Augusta, Georgia [Master's thesis]: Columbia, University of South Carolina, 94 p.

Maher, H. D., Jr., 1987a, Kinematic history of mylonitic rocks from the Augusta fault zone, South Carolina and Georgia: *American Journal of Science*, **287**, 795-816.

Maher, H. D. 1987b. D_3 folding in the eastern Piedmont associated with Alleghanian thrusting. In: *Anatomy of the Alleghanian orogeny as seen from the Piedmont of South Carolina and Georgia* (edited by Secor, D. T., Jr.). Columbia, South Carolina Geological Survey, Carolina Geological Society Field Trip Guidebook for 1987, 35-48.

Maher, H. D., Jr., and Sacks, P. E., 1987, Geologic map of the Clarks Hill and Leah Quadrangles, SC & GA, *in* Secor, D. T., Jr., ed., Anatomy of the Alleghanian orogeny as seen from the Piedmont of South Carolina and Georgia: Columbia, South Carolina Geological Survey, Carolina Geological Society 50th Anniversary Meeting, pl. 1, scale 1 : 40,000, 1 sheet.

Maher, H. D., Palmer, A. R., Secor, D. T., and Snoke, A. W., 1981, New trilobite locality in the Piedmont of South Carolina, and its regional implications: *Geology*, **9**, 34-36.

Maher, H. D., Sacks, P. E., and Secor, D. T., Jr., 1991, The eastern Piedmont in South Carolina, *in* Horton, J. W., Jr., and Zullo, V. A., eds., The geology of the Carolinas: Knoxville, The University of Tennessee Press, p. 93-108.

Maher, H. D., Jr., Dallmeyer, R. D., Secor, D. T., Jr., and Sacks, P. E., 1994, $^{40}Ar/^{39}Ar$ constraints on chronology of Augusta fault zone movement and late Alleghanian extension, southern Appalachian Piedmont, South Carolina and Georgia: *American Journal of Science*, **294**, 428-448.

Mauldin, J.C., Shervais, J.W., and Dennis, A.J. (this volume) Petrology and geochemistry of metavolcanic rocks from a Neoproterozoic volcanic arc, Savannah River Site, South Carolina, *in* Bartholomew, J. (ed) *Basement terranes of beneath the SE Atlantic Coastal Plain, Georgia and South Carolina*: Geological Society of America Special Paper, in press.

Mueller, P.A., Heatherington, A.L., Wooden, J.L., Shuster, R.D., Nutman, A.P., and Williams, I.S., 1994, Precambrian zircons from the Florida basement: a Gondwana connection, *Geology*, **22**, 119-122.

Nance, R.D., Murphy, J.B., Strachan, R.A., D'Lemos, R.S., Taylor, G.K., 1991, Late Proterozoic tectonostratigraphic evolution of the Avalonian and Cadomian terranes, Precambrian Geology, 53, 41-78.

Nance, R.D., and Murphy, J.B., 1996, Basement isotopic signatures and Neoproterozoic paleogeography of the Avalonian-Cadomian and related terranes in the circum North Atlantic, in Nance, R. D., and Thompson, M., eds., Avalonian and related peri-Gondwanan terranes of the circum-North Atlantic: Geological Society of America Special Paper 304, 333-346.

Potts, P.J., Tindle, A.G., and Webb, P.C., 1992, Geochemical reference material compositions; CRC Press, Boca Raton FL, 313 pp.

Pouchou J-L, and Pichoir F., 1991, Quantitative analysis of homogeneous or stratified microvolumes applying the model "PAP". In: KFJ Heinrich, DE Newbury (eds) Electron Probe Quantitation, p 31-76 Plenum Press, New York.

Pray, J. R., 1993, U-Pb geochronology of the Modoc shear zone and adjacent terranes in the southeastern Appalachian Piedmont. Unpublished M.S. thesis, Department of Geological Sciences, University of South Carolina, Columbia, South Carolina, 35 p.

Pray, J. R., 1997, Geology of the Modoc fault zone and adjacent terranes in the southern Appalachian Piedmont: Geochronologic and kinematic investigations [unpublished PhD dissertation], Columbia: University of South Carolina, 94 pp.

Roden, M.F., LaTour, T.E., Capps, C., and Whitney, J.A., 1997, Incomplete metamorphic equilibration in a metadiorite from crystalline basement of the Savannah River Site, *Geological Society of America Abstracts with Programs,* **29/3,** 25.

Rogers, J. J. W., 1982, Criteria for recognizing environments of formation of volcanic suites; Application of these criteria to volcanic suites in the Carolina slate belt: *in* Bearce, D. N., Black, W. W., Kish, S. A., and Tull, J. F., eds., Tectonic studies in the Talladega and Carolina slate belts, southern Appalachian orogen: *Geological Society of America, Special Paper 191*, 99-107.

Sacks, P. E. & Dennis, A. J., 1987, The Modoc zone - D_2 (early Alleghanian) in the eastern Appalachian Piedmont, South Carolina and Georgia. In: *Anatomy of the Alleghanian orogeny as seen from the Piedmont of South Carolina and Georgia* (edited by Secor, D. T., Jr.). Columbia, South Carolina Geological Survey, Carolina Geological Society Field Trip Guidebook for 1987, 19-34.

Sacks, P. E., Maher, H. D., Jr., Secor, D. T., Jr., and Shervais, J. W., 1989, The Burks Mountain Complex, Kiokee belt, Southern Appalachian Piedmont of South Carolina and Georgia, *in* Mittwede, S. K., and Stoddard, E. F., eds., Ultramafic rocks of the Appalachian Piedmont: *Geological Society of America Special Paper 231*, 75-86.

Samson, S., Palmer, A. R., Robison, R. A., and Secor, D. T., Jr., 1990, Biogeographical significance of Cambrian trilobites from the Carolina slate belt: *Geological Society of America Bulletin*, **102**, 1459-1470.

Secor, D. T., Jr., and Snoke, A. W., 1978, Stratigraphy, structure and plutonism in the central South Carolina Piedmont, *in* Snoke, A. W., ed., Geological investigations of the eastern Piedmont,

southern Appalachians: Columbia, South Carolina Geological Survey, Carolina Geological Society Field Trip Guidebook for 1978, 65-123.

Secor, D. T., Jr., Peck, L. S., Pitcher, D. M., Prowell, D. C., Simpson, D. H., Smith, W. A., and Snoke, A. W., 1982, Geology of the area of induced seismic activity at Monticello Reservoir, South Carolina: *Journal of Geophysical Research, Part B*, **87**, 6945-6957.

Secor, D. T., Jr., Samson, S. L., Snoke, A. W., and Palmer, A. R., 1983, Confirmation of the Carolina slate belt as an exotic terrane: *Science*, **221**, 649-650.

Secor, D. T. Jr., Snoke, A. W., Bramlette, K. W., Costello, O. P., and Kimbrell, O. P., 1986a, Character of the Alleghanian orogeny in the southern Appalachians: Part I. Alleghanian deformation in the eastern Piedmont of South Carolina: *Geological Society of America Bulletin*, **97**, 1319-1328.

Secor, D. T., Jr., Snoke, A. W., and Dallmeyer, R. D., 1986b, Character of the Alleghanian orogeny in the southern Appalachians: Part III. Regional tectonic relations: *Geological Society of America Bulletin*, **97**, 1345-1353.

Shelley, S. A., 1988, Geochemical characterization of metavolcanics from the Carolina slate belt, south-central South Carolina [Masters thesis]: Columbia, University of South Carolina, 81 p.

Shervais, J. W., Shelley, S. A., and Secor, D. T., Jr., 1996, Geochemistry of volcanic rocks of the Carolina and Augusta Terranes in central South Carolina: An exotic rifted volcanic arc?, *in* Nance, R. D., and Thompson, M., eds., Avalonian and related peri-Gondwanan terranes of the circum-North Atlantic: *Geological Society of America Special Paper 304*, 219-236.

Snipes, D.S., Fallaw, W.C., Price, Van, and Cumbest, R.J. (1993) The Pen Branch fault: Documentation of late Cretaceous-Tertiary faulting in the coastal plain of South Carolina, Southeastern Geology, 33, 195-218.

Snoke, A.W., and Frost, R. B., 1990, Exhumation of high pressure pelitic schist, Lake Murray Spillway, South Carolina: Evidence for crustal extension during Alleghanian strike-slip faulting: *American Journal of Science*, **290**, 853-881.

Snoke, A. W., Kish, S. A., and Secor, D. T., Jr., 1980, Deformed Hercynian granitic rocks from the Piedmont of South Carolina: *American Journal of Science*, **280**, 1018-1034.

Taggart, J.E., Lindsay, J.R., Scott, B.A., Vivit, D.V., Bartel, A.J., and Stewart, K.C. (1987) Analysis of geologic materials by wavelength dispersive X-ray fluorescence spectrometry; U.S. Geological Survey Professional Paper 1770, E1-E19.

Whitney, J. A., Paris, T. A., Carpenter, R. H., and Hartley, M. E., III, 1978, Volcanic evolution of the southern slate belt of Georgia and South Carolina: a primitive oceanic island arc: *Journal of Geology*, **86**, 173-192.

Williams, H., and Hatcher, R. D., Jr., 1982, Suspect terranes and accretionary history of the Appalachian orogen: *Geology*, **10**, 530-536.

Williams, H., and Hatcher, R. D., Jr., 1983, Appalachian suspect terranes: *in* Hatcher, R. D., Jr., Williams, H., and Zietz, I., eds., Contributions to the tectonics and geophysics of mountain chains: *Geological Society of America Memoir 158*, 33-53.

Wright, J. E., and Seiders, V. M., 1980, Age of zircon from volcanic rocks of the central North Carolina Piedmont and tectonic implications for the Carolina volcanic slate belt: *Geological Society of America Bulletin*, **91**, 287-294.

Figure Captions

Figure 1. Provisional terrane map of the eastern Piedmont in South Carolina, Georgia, and Alabama (modified in part after Horton and others, 1991, with additional data from West and others, 1995, Dennis and Wright, 1997, and Dennis and Shervais, 1996). Carolina terrane includes Carolina slate belt, the Charlotte belt, the Kings Mountain belt, and the putative Juliette "non-terrane". The Kiokee belt, Uchee belt, and Dreher Shoals subterrane comprise the newly defined KUDZU terrane. CPS = Central Piedmont Suture.

Figure 2. Geologic map showing the distribution of crystalline basement lithologic units in and around the Savannah River Site and National Laboratory. Major units beneath the Savannah River Site include the Crackerneck Metavolcanic Complex (low-grade metavolcanic rocks), the Deep Rock Metavolcanic Complex (epidote-amphibolite grade metavolcanic rocks), the DRB Plutonic Suite, the Pen Branch Metavolcanic Complex (amphibolite to lower granulite grade metavolcanic rocks), PBF Plutonic Suite, and clastic sedimentary rocks of the Triassic Dunbarton basin. Triassic-Jurassic mafic igneous complex south of the Dunbarton basin is based on aeromagnetic anomalies; core data from wells C-7 and C-10 indicate that much of this basement is pinked granite of the PBF Plutonic Suite. Subsurface extents of the Devonian Springfield pluton and the Carboniferous Graniteville pluton are based on gravity anomalies. The Graniteville pluton is sampled by core from well C-2 and in limited surface exposures (outlined on map). The Springfield pluton is sampled by well SAL-1. AFZ = Augusta fault zone, EPFS = Eastern Piedmont Fault System.

Figure 3. Photomicrographs of DRB metadiorites: (a) Relict igneous hornblende (brown) surrounded by mantle of metamorphic blue-green amphibole (UPL); (b) Primary igneous zoning and albite twinning in relict plagioclase porphyroclast (UXN). Field of view 2.3 mm in both.

Figure 4. Ca-Mg-Fe plot showing compositions of metamorphic and relict igneous amphiboles in metaplutonic rocks of the DRB and PBF plutonic suites.

Figure 5. Tetrahedral aluminum afu vs titanium afu (atomic formula units) in metamorphic and relict igneous amphiboles of the DRB and PBF plutonic suites, based on 23 oxygens. Relict igneous hornblende (❑) is higher in Ti and lower in Al^{IV} than coexisting metamorphic amphibole (diamonds) in metadiorites of DRB plutonic suite. Metagranitoids of the PBF plutonic suite contain no relict igneous hornblende, but the metamorphic blue-green amphibole (△) is higher in Ti than metamorphic amphibole in the DRB metadiorites, suggesting higher equilibration temperatures.

Figure 6. Plagiclase compositions in DRB metadiorites and PBF metagranitoids. DRB plagioclase = ✳, PBF unpinked plagioclase = ❑, PBF partially pinked gneiss = △, PBF thoroughly pinked granites = ▲.

Figure 7. Photomicrographs of PBF metagranitoids: (a) Microcline with characteristic tartan twinning in quartz-plagioclase-amphibole granite (UXN); (b) Metamorphic amphibole (extinct) intergrown with quartz, plagioclase, and k-feldspar (UXN). Field of view 2.3 mm in both.

Figure 8. Plutonic rock compositions based on normative mineralogy in the quartz-alkali feldspar-plagioclase ternay: (a) metaplutonic rocks of the DRB plutonic suite (■) are low in both quartz and alkali feldspar; compositions range from diorite to tonalite, but most are quartz diorites; (b) normal (i.e., not "pinked") metaplutonic rocks of the PBF plutonic suite (filled diamonds) are low in quartz but have slightly higher normative and alkali feldspar than the DRB diorites; most are quartz monzodiorites. "Pinked" PBF metagranitoids (unfilled diamonds) are high in both quartz and alkali feldspar, and plot within the "Granite" field.

Figure 9. Harker diagrams for DRB and PBF metaplutonic rocks. DRB diorites = ■, unpinked PBF quartz monzodiorites = ▲, pinked PBF granites = ▼. Solid lines indicate anhydrous fractionation paths calculated with the program COMAGMAT (Ariskin and others, 1994).

Figure 10. AFM diagrams for (a) DRB metadiorites and (b) PBF metagranitoids, with calc-alkaline / tholeiite dividing line of Irvine and Barager (1974). DRB diorites = ■, unpinked PBF quartz monzodiorites = filled diamonds, pinked PBF granites = open diamonds.

Figure 11. Chondrite-normalized REE plots for metaplutonic rocks of DRB and PBF intrusive complexes. PBF metagranitoids have higher total REE and higher La/Lu than DRB metadiorites. Note large negative Eu anomaly in pinked granodiorite.

Appendix 1: Formal Description of New Units Defined in the Publication

All of the units defined here are exposed in core obtained from deep wells in and around the Savannah River Site. Core is stored at the SRS Core Repository. Well locations are shown in figure 2 of this report, and listed below in UTM coordinates, SE USA baseline.

DRB Plutonic Suite

Named for the the DRB-1 well in which it occurs. All DRB (Deep Rock Borehole) core is 4" in diameter. Because basement was the target of this core series, thousands of feet of core are available for study.

Type section: Core DRB-1; Northing: 3684171 Easting: 437524.7, Total Depth: 1904'

Description: footage 892'-1904': Diorite and quartz diorite gneiss, with common hornblende porphyroclasts in finer-grained, foliated groundmass of quartz, plagioclase, amphibole, and chlorite. Minor intercalated metavolcanics and cross-cutting amphibolite dikes.

PBF Plutonic Suite

Named for the PBF well series in which it principally occurs. All PBF core is 2.5" in diameter.

Type section: Core PBF-7, Northing: 3678485 Easting: 442463.6, Total Depth:

Description: footage 2550' to 3100': Unpinked, foliated granodiorite gneiss.

footage 3140' to 3480': Transition zone, unpinked granodiorite and diorite gneiss with some partly pinked granodiorite gneiss.

footage 3500' to 3600': Pinked granitic gneiss. Lower contact at 3600' is mylonite zone which separates PBF plutonic suite from high-grade metavolcanic rocks of the Pen Branch Metavolcanic Complex.

Reference section #1: Seismic Attenuation Core, Northing: 3679655 Easting: 440618

Description: footage 1078'-1118': Pinked granitic gneiss.

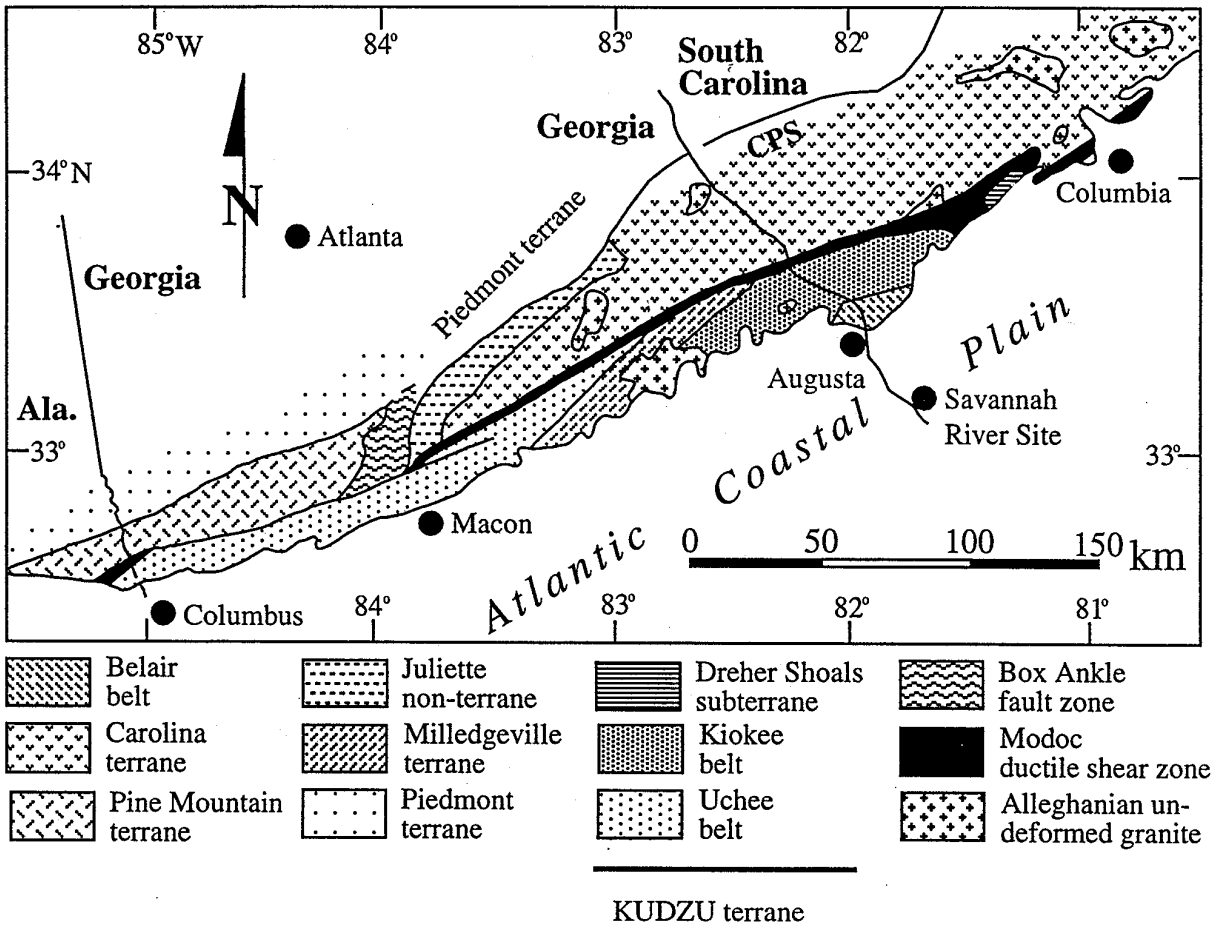

Figure 1. Provisional terrane map of the eastern Piedmont in South Carolina, Georgia, and Alabama (modified in part from Horton et al., 1991, with additional data from West and others, 1995, Dennis and Wright, 1997, and Dennis and Shervais, 1996). CPS = Central Piedmont Suture.

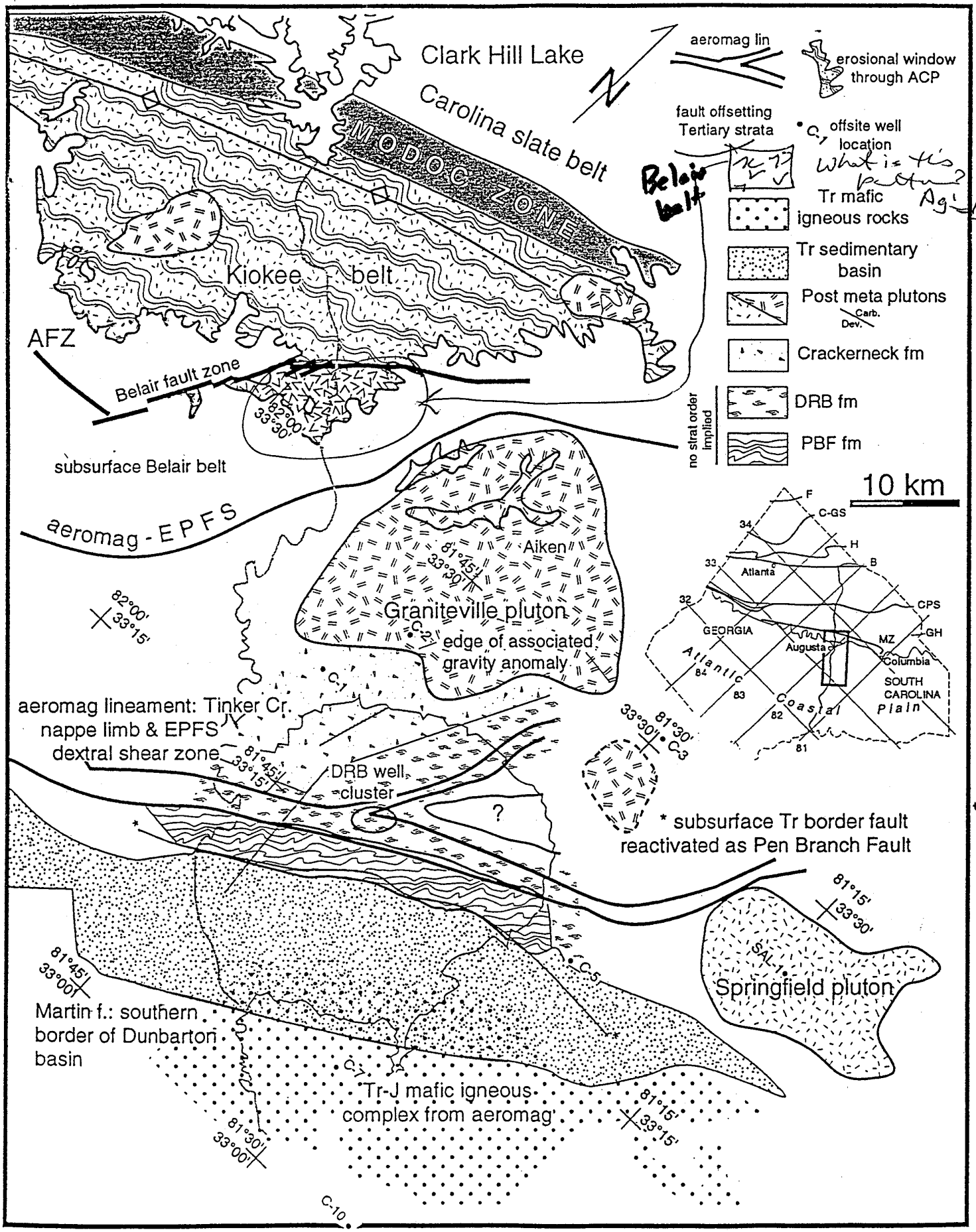
Clark Hill Lake
Carolina slate belt
MODOC ZONE
Kiokee belt
AFZ
Belair fault zone
subsurface Belair belt
aeromag - EPFS
aeromag lin
erosional window through ACP
fault offsetting Tertiary strata
offsite well location
Tr mafic igneous rocks
Tr sedimentary basin
Post meta plutons
Carb.
Dev.
Crackerneck fm
DRB fm
PBF fm
no strat order implied
10 km
Aiken
Graniteville pluton
edge of associated gravity anomaly
aeromag lineament: Tinker Cr. nappe limb & EPFS dextral shear zone
DRB well cluster
* subsurface Tr border fault reactivated as Pen Branch Fault
Springfield pluton
Martin f.: southern border of Dunbarton basin
Tr-J mafic igneous complex from aeromag
82°00'
33°30'
81°45'
33°15'
33°30'
81°30'
81°15'
33°30'
81°45'
33°00'
81°30'
33°00'
81°15'
33°15'
F
C-GS
H
B
Atlanta
CPS
GH
MZ
Augusta
Columbia
GEORGIA
SOUTH CAROLINA
Atlantic Coastal Plain
34
33
32
84
83
82
81

Fig 2

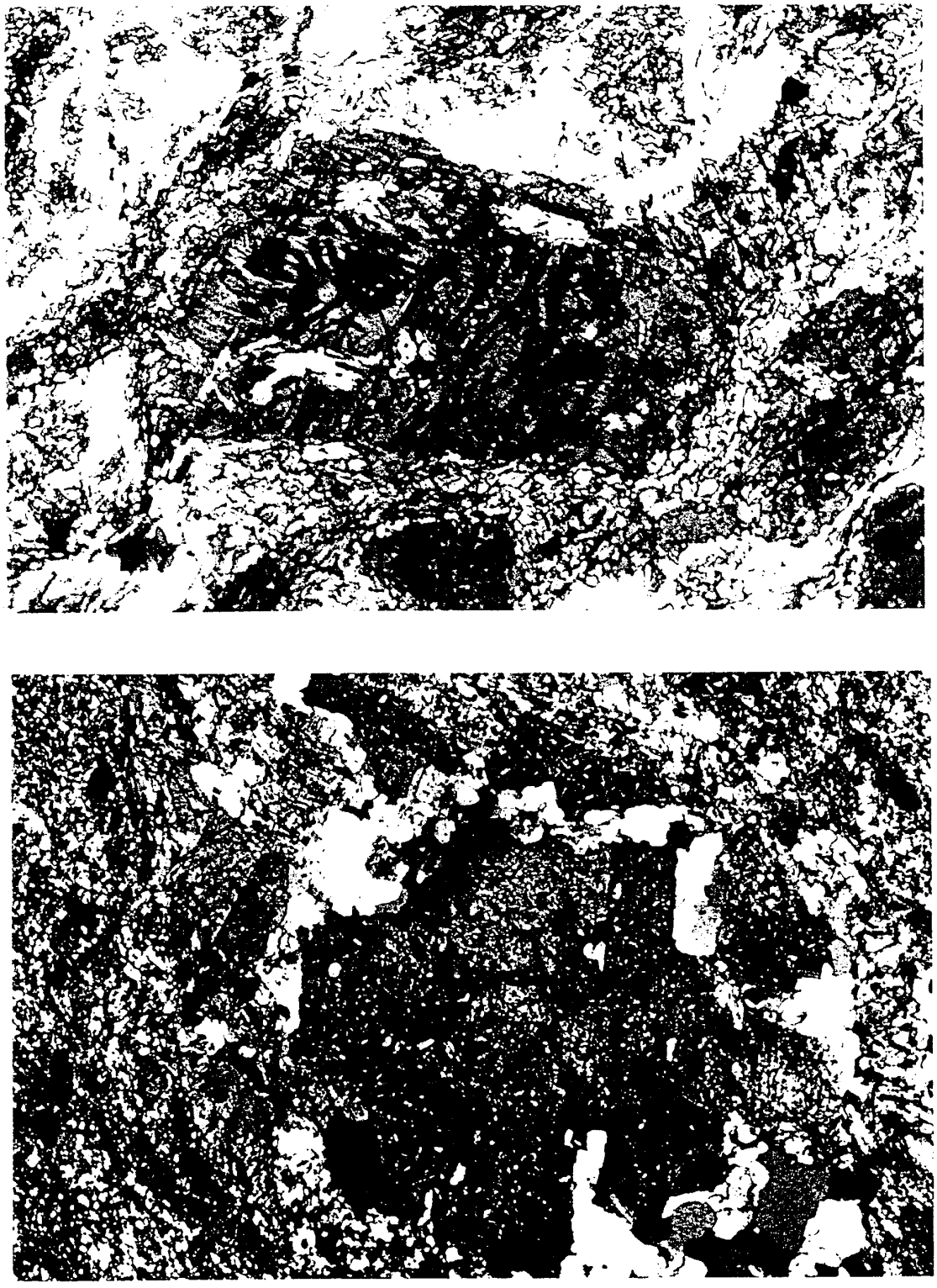

Figure 13. Photomicrographs of DRB metadiorites: (a) Relict igneous hornblende (brown) surrounded by mantle of metamorphic blue-green amphibole (UPL); (b) Primary igneous zoning and albite twinning in relict plagioclase porphyroclast (UXN). Field of view 5.6 mm in both.

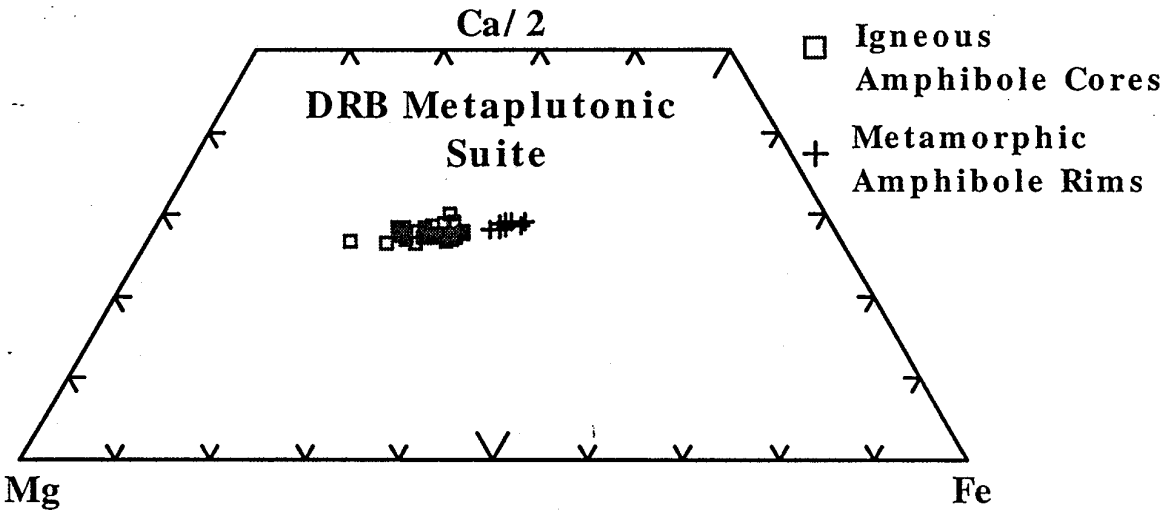
Ca/ 2
DRB Metaplutonic Suite
Igneous Amphibole Cores
Metamorphic Amphibole Rims
Mg
Fe

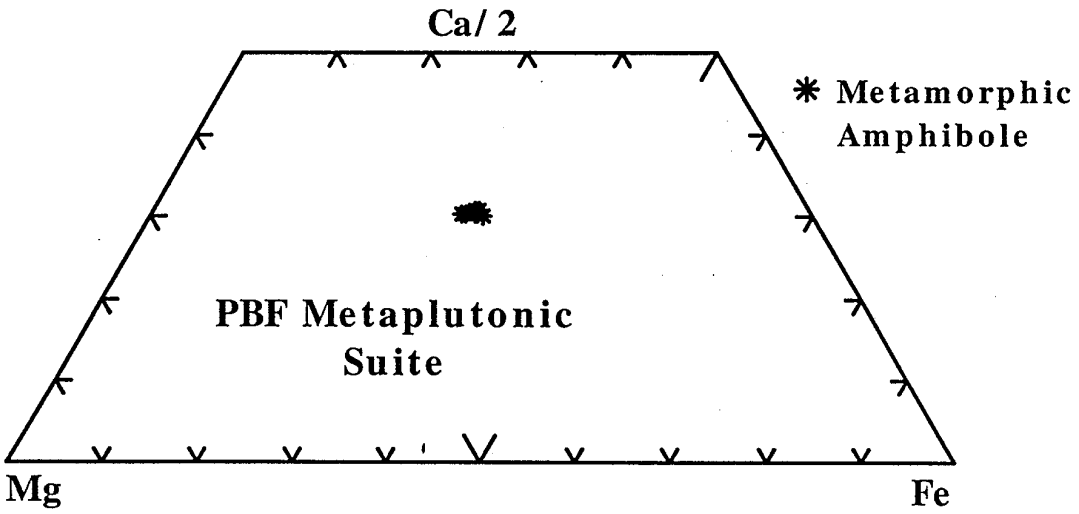
Ca/ 2
Metamorphic Amphibole
PBF Metaplutonic Suite
Mg
Fe

Fig. 5

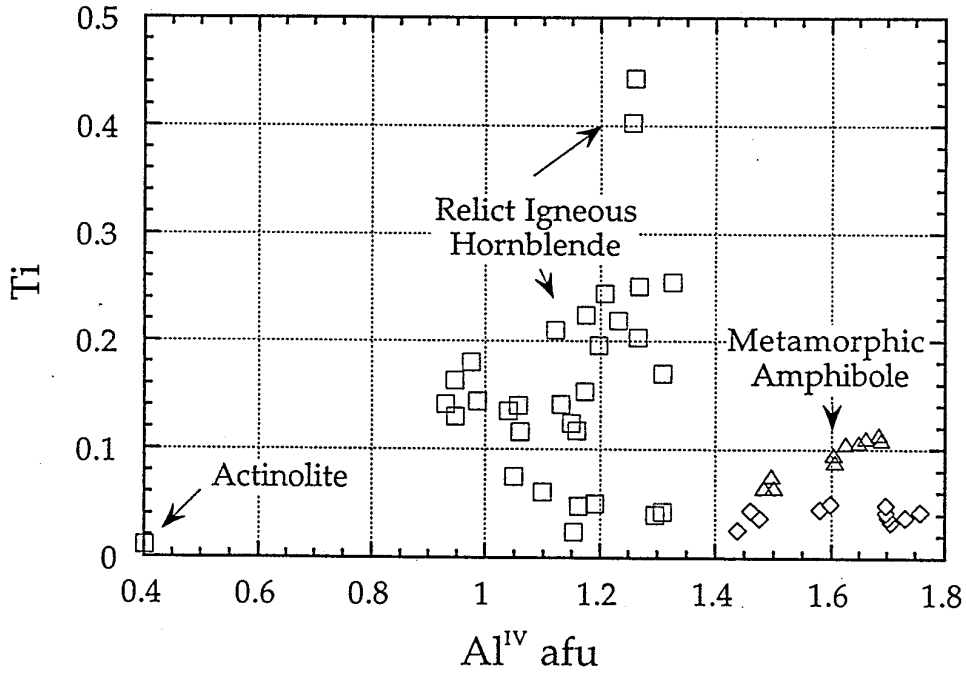
0.5
0.4
0.3
0.2
0.1
0
Ti
Relict Igneous
Hornblende
Metamorphic
Amphibole
Actinolite
0.4
0.6
0.8
1
1.2
1.4
1.6
1.8
Al^IV afu

Fig. 6

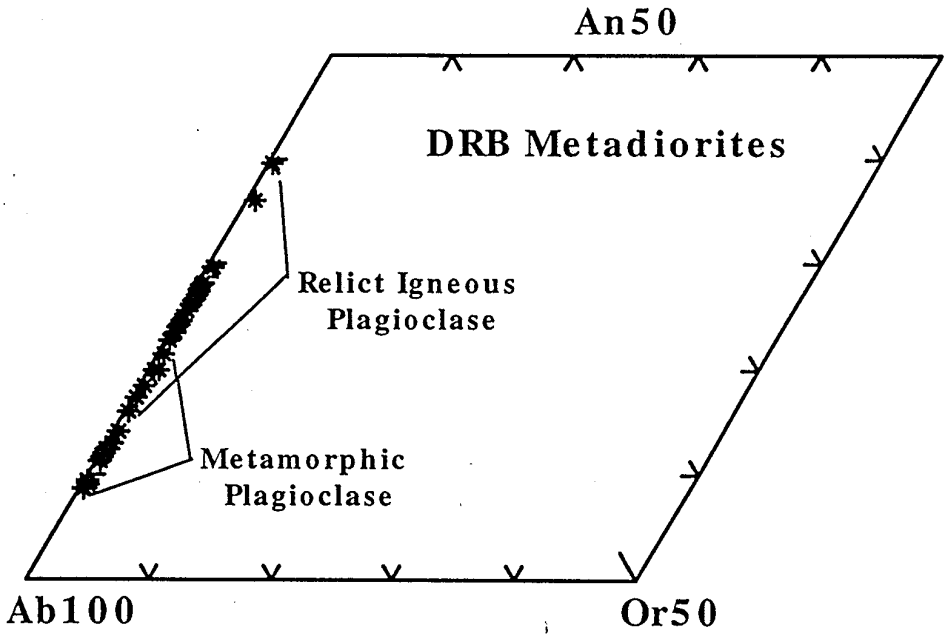
An50
DRB Metadiorites
Relict Igneous Plagioclase
Metamorphic Plagioclase
Ab100
Or50

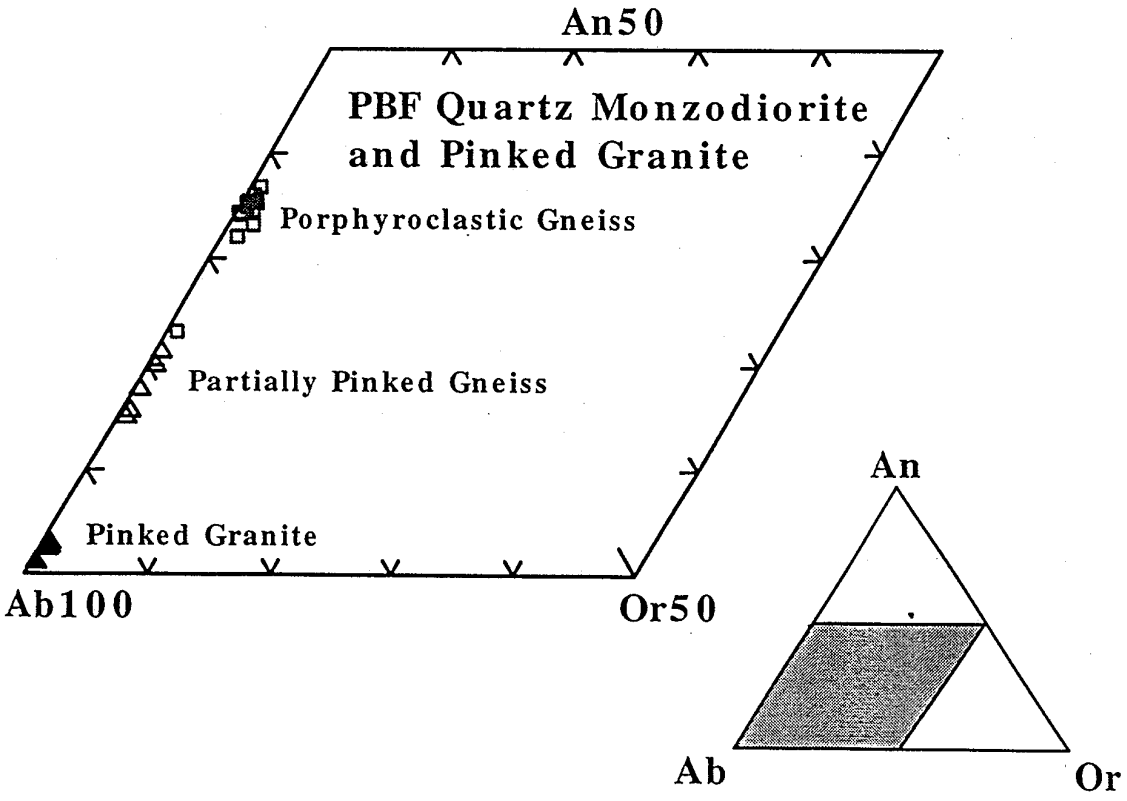
An50
PBF Quartz Monzodiorite and Pinked Granite
Porphyroclastic Gneiss
Partially Pinked Gneiss
Pinked Granite
Ab100
Or50
An
Ab
Or

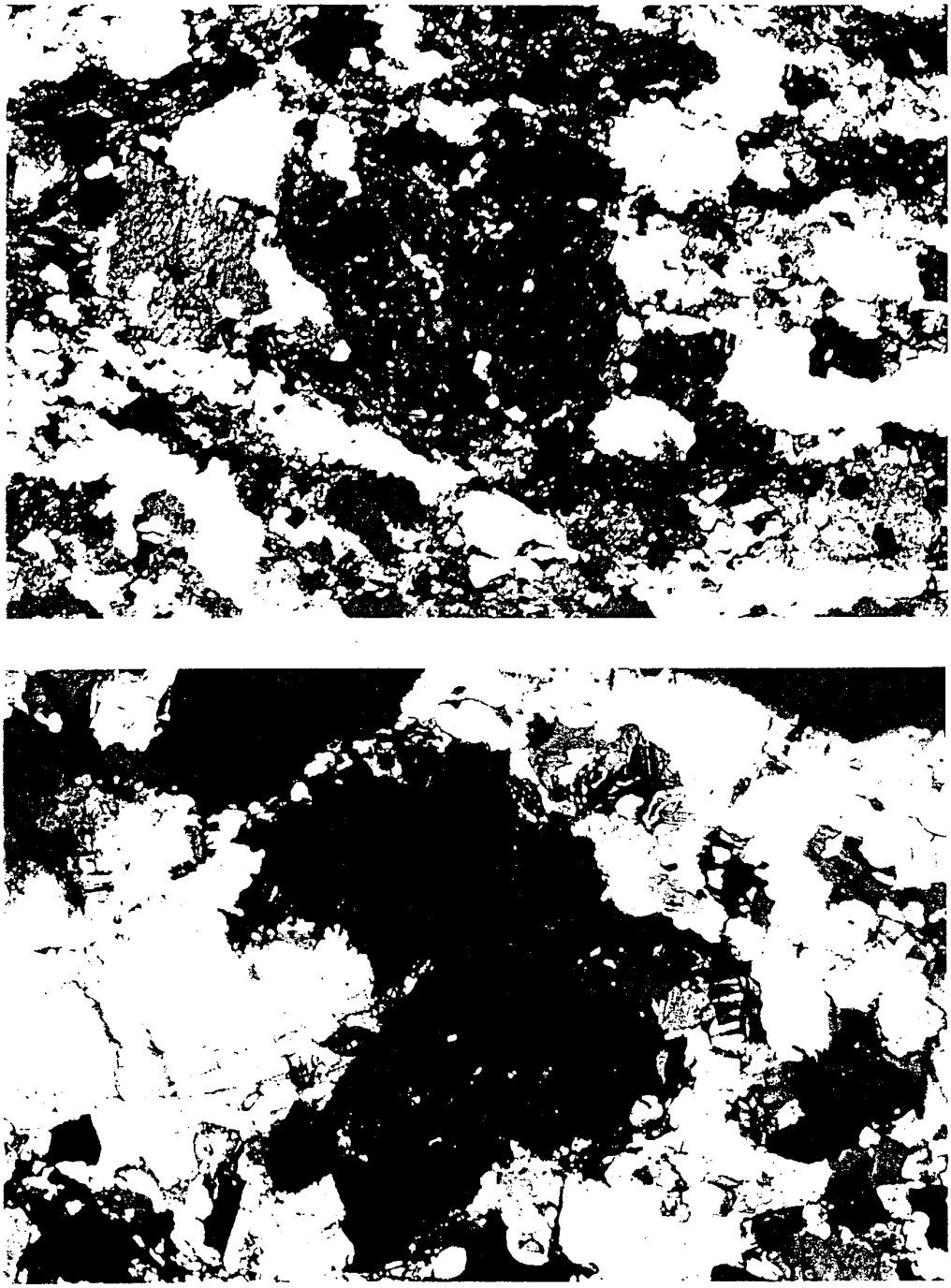

~~Plate 18~~ Fig 7 Photomicrograph of amphibole porphyroclasts within PBF formation metagranodiorites. (Upper : Unaltered metamorphic amphibole in PBF quartz monzodiorite. PBF7-107, Lower: Chloritized amphibole in "Pinked" PBF formation granodiorite. PBF7-159).

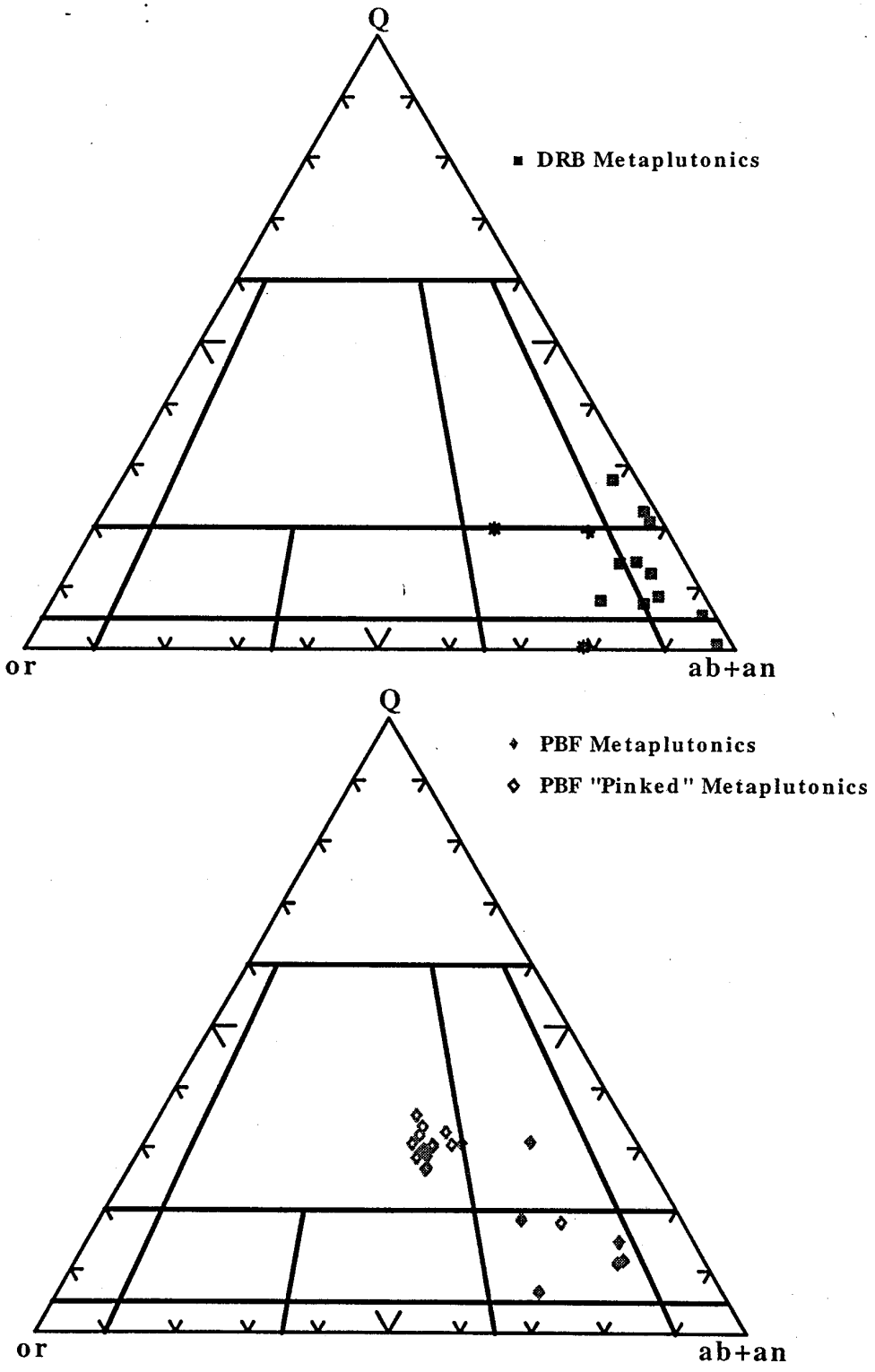

Figure 8
Shervais et al, 1998

Fig. 9

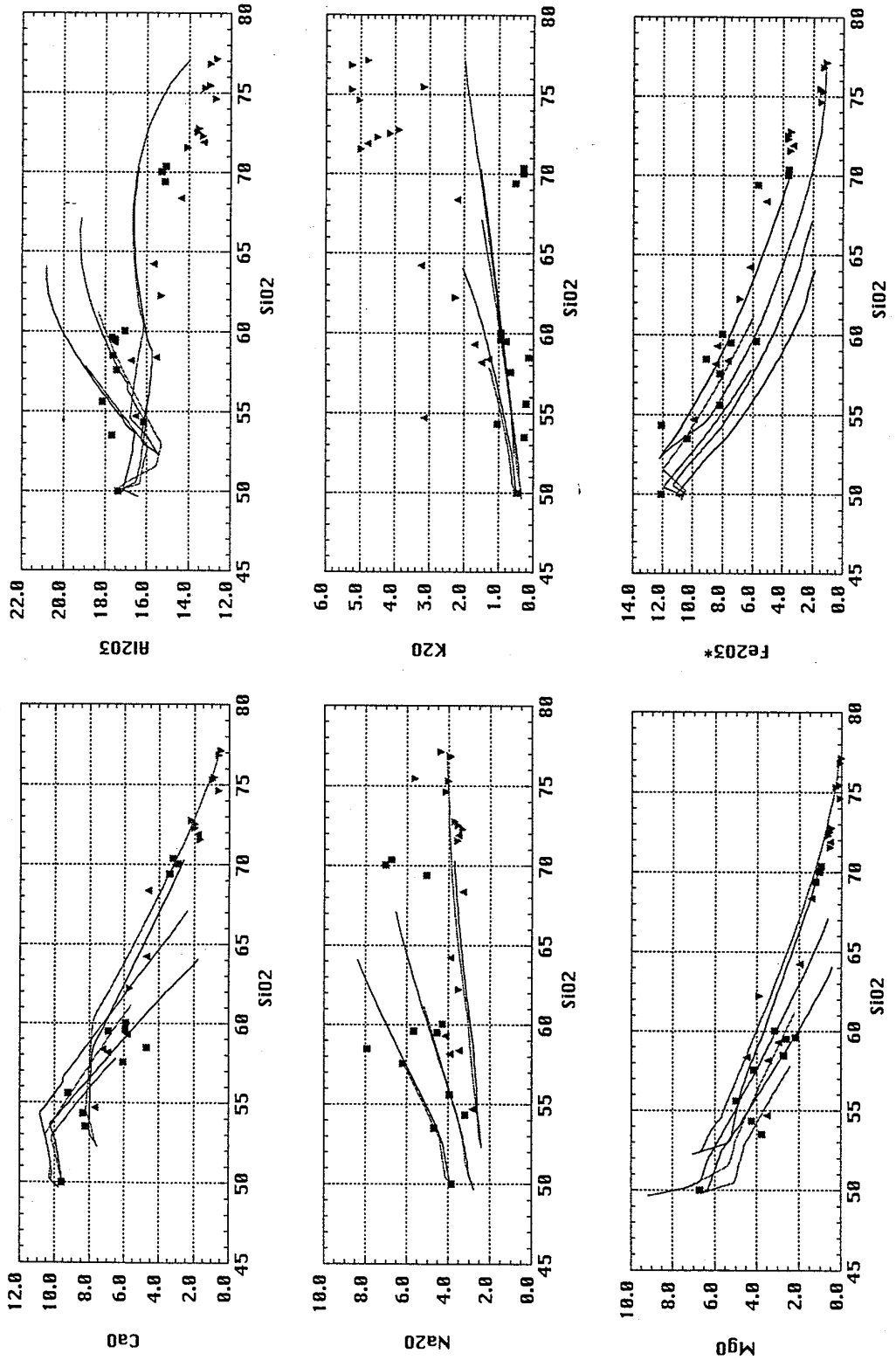

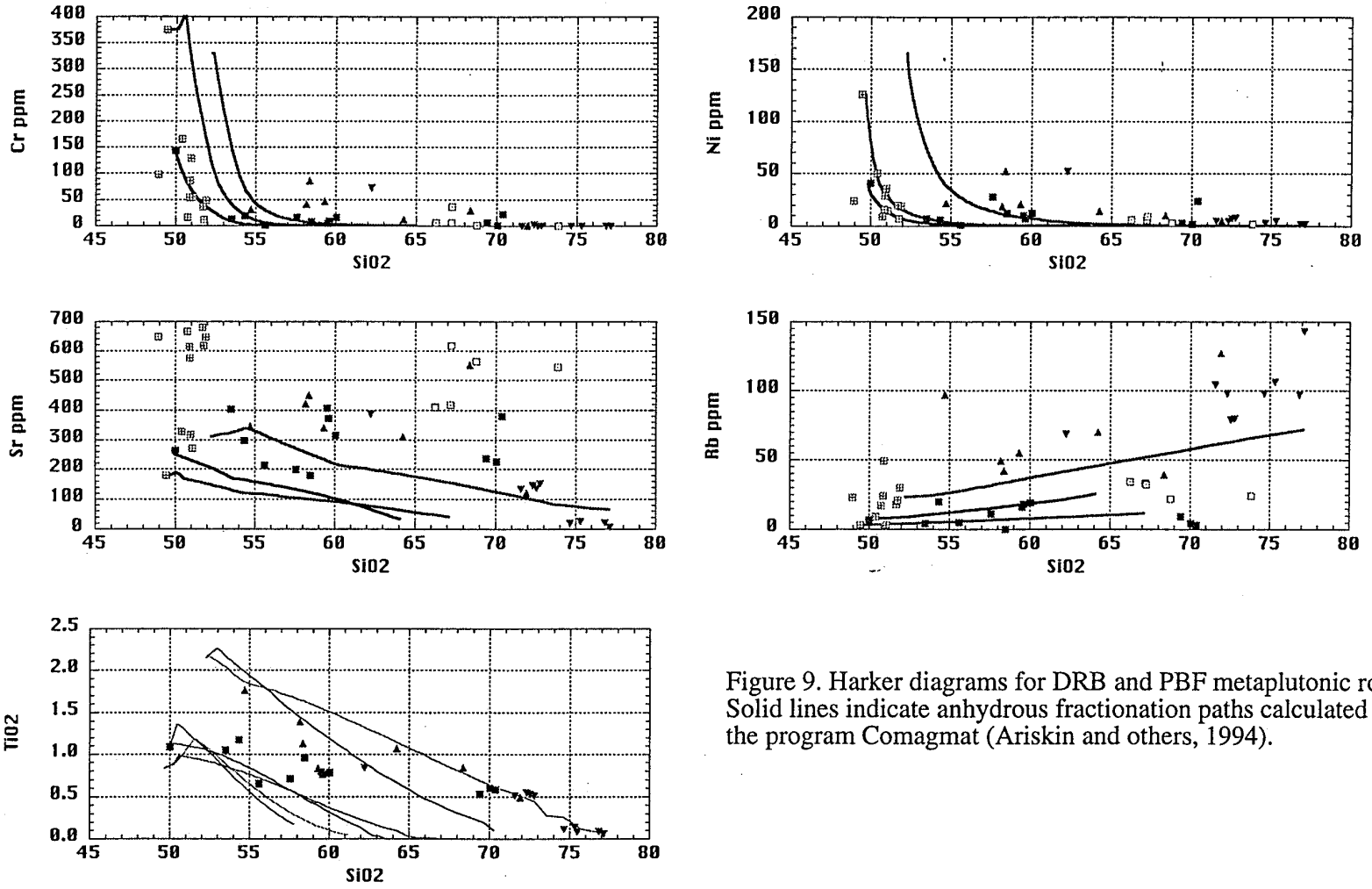

Figure 9. Harker diagrams for DRB and PBF metaplutonic rocks. Solid lines indicate anhydrous fractionation paths calculated with the program Comagmat (Ariskin and others, 1994).

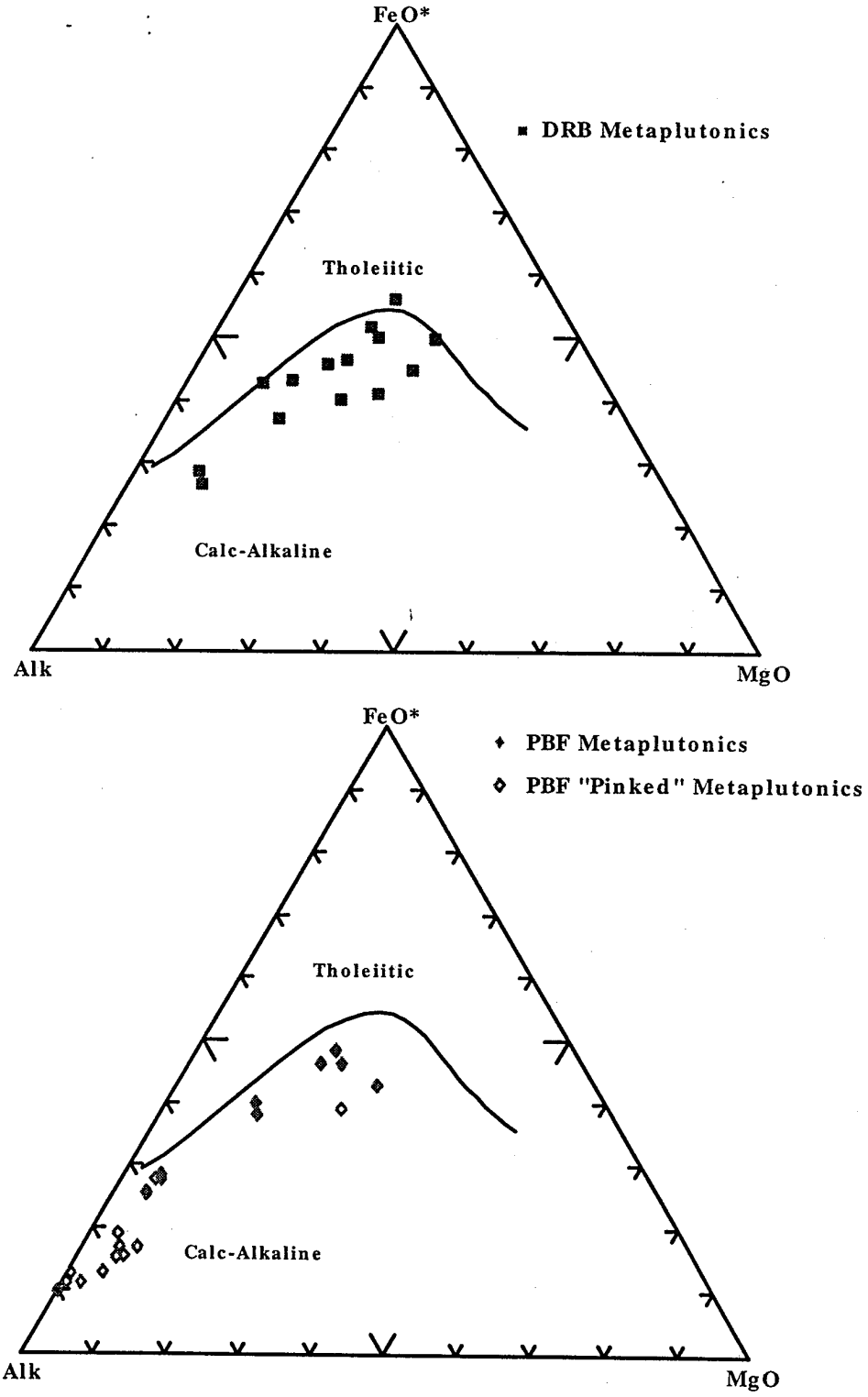

Figure 10
Shervais et al, 1998

Fig 11

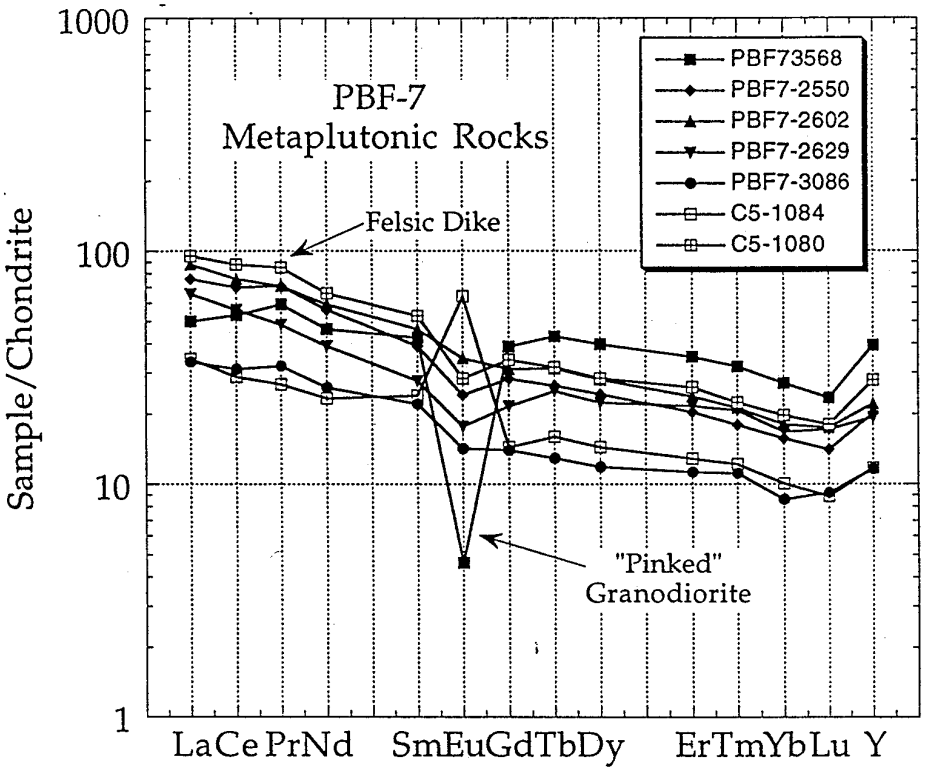
PBF-7
Metaplutonic Rocks
PBF73568
PBF7-2550
PBF7-2602
PBF7-2629
PBF7-3086
C5-1084
C5-1080
Felsic Dike
"Pinked"
Granodiorite
Sample/Chondrite
1000
100
10
1
LaCePrNd SmEuGdTbDy ErTmYbLu Y

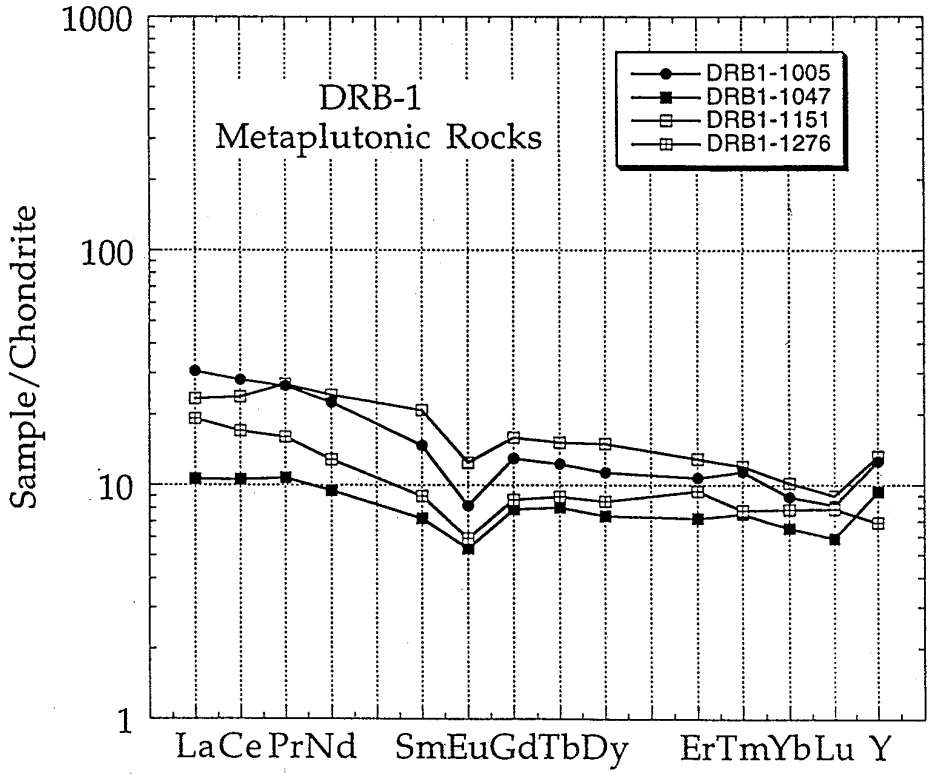
DRB-1
Metaplutonic Rocks
DRB1-1005
DRB1-1047
DRB1-1151
DRB1-1276
Sample/Chondrite
1000
100
10
1
LaCePrNd SmEuGdTbDy ErTmYbLu Y

Table 1a. Representative amphibole analyses.

Sample#	DRB-1-153 Metamorphic rim	DRB-1-153 Metamorphic rim	DRB-1-153 Metamorphic rim	DRB-1-153 Metamorphic rim	DRB-1-153 Metamorphic rim	DRB-1-153 Metamorphic rim	DRB-1-153 Relict Igneous core	DRB-1-153 Relict actinolite	DRB-1-153 Relict Igneous core
SiO2	46.36	48.35	47.37	48.20	46.33	47.69	43.40	53.06	43.65
TiO2	2.02	1.28	1.30	1.48	1.77	1.17	0.41	0.10	0.39
Al2O3	8.71	7.23	7.42	7.16	9.21	7.54	12.93	3.69	12.28
Cr2O3	0.00	0.00	0.00	0.00	0.01	0.01	0.00	0.00	0.00
MgO	12.60	13.69	13.01	14.34	13.39	12.72	10.10	16.41	10.24
CaO	11.28	11.22	11.25	11.08	11.22	11.10	10.89	11.75	11.16
MnO	0.34	0.37	0.39	0.39	0.32	0.38	0.36	0.41	0.36
FeO	15.10	14.31	14.99	13.29	13.58	15.13	17.29	11.76	17.44
Na2O	1.22	1.11	1.09	1.11	1.33	1.13	1.69	0.57	1.63
K2O	0.19	0.18	0.19	0.16	0.19	0.17	0.36	0.04	0.37
Total	97.82	97.74	97.02	97.21	97.35	97.03	97.43	97.78	97.52

Sample#	DRB-1-153 Relict Igneous core	DRB-1-153 Relict Igneous core	DRB-1-153 Relict Igneous core	DRB-1-153 Relict Igneous core	DRB-1-153 Relict Igneous core	DRB-1-59 Relict Igneous core	DRB-1-59 Relict Igneous core	DRB-1-59 Relict Igneous core	DRB-1-59 Relict Igneous core
SiO2	45.33	43.37	43.74	43.30	46.34	41.76	45.05	41.53	41.18
TiO2	0.30	0.39	0.32	0.33	0.22	0.37	0.38	0.38	0.32
Al2O3	10.04	13.48	12.33	12.48	9.95	14.89	11.62	15.18	15.40
Cr2O3	0.00	0.00	0.01	0.00	0.00	0.00	0.00	0.01	0.00
MgO	10.88	10.04	10.31	10.07	11.92	8.87	10.75	8.61	8.40
CaO	11.48	11.03	10.96	10.95	11.75	10.89	10.97	11.00	10.81
MnO	0.29	0.34	0.35	0.34	0.30	0.42	0.39	0.44	0.37
FeO	17.24	16.86	17.30	17.49	15.62	18.07	16.79	17.88	18.25
Na2O	1.29	1.71	1.65	1.61	1.26	1.80	1.49	1.85	1.88
K2O	0.28	0.32	0.37	0.44	0.24	0.39	0.31	0.40	0.38
Total	97.13	97.54	97.35	97.01	97.59	97.45	97.75	97.29	96.99

Sample#	DRB-1-59 Relict Igneous core	DRB-1-59 Relict Igneous core	DRB-1-59 Relict Igneous core	DRB-1-59 Metamorphic rim	DRB-1-59 Metamorphic rim	DRB-1-59 Metamorphic rim	DRB-1-59 Metamorphic rim	DRB-1-41 Relict Igneous core	DRB-1-41 Relict Igneous core
SiO2	41.53	42.23	42.05	46.91	42.17	45.22	46.32	46.00	45.94
TiO2	0.34	0.44	0.40	1.21	7.43	2.24	1.18	0.45	0.43
Al2O3	15.26	15.04	15.53	8.02	9.93	9.23	9.52	10.48	9.98
Cr2O3	0.00	0.00	0.02	0.00	0.00	0.00	0.01	0.03	0.02
MgO	8.79	8.71	8.57	12.22	10.42	12.34	12.00	11.23	11.34
CaO	10.82	10.95	10.88	10.97	10.28	11.05	10.92	11.03	11.07
MnO	0.44	0.41	0.41	0.40	0.38	0.41	0.40	0.26	0.23
FeO	18.04	18.23	17.87	16.19	15.37	14.77	15.77	16.62	16.36
Na2O	1.80	1.90	1.87	1.24	1.40	1.32	1.45	1.39	1.59
K2O	0.40	0.43	0.39	0.20	0.22	0.24	0.23	0.21	0.24
Total	97.42	98.33	97.99	97.35	97.61	96.81	97.81	97.68	97.19

Table 1a. Representative amphibole analyses.

Sample#	DRB-1-41 Relict Igneous core	DRB-1-41 Metamorphic rim	DRB-1-41 Metamorphic rim	DRB-1-41 Metamorphic rim	DRB-1-41 Metamorphic rim	DRB-1-41 Metamorphic rim	DRB-1-41 Metamorphic rim	DRB-1-60 Relict Igneous core	DRB-1-60 Relict Igneous core
SiO2	48.59	45.86	45.98	46.08	45.18	46.37	46.57	44.35	47.51
TiO2	0.97	1.33	2.82	1.79	1.58	1.11	1.89	0.38	0.69
Al2O3	7.03	10.11	8.76	9.16	10.08	9.57	8.43	12.74	9.32
Cr2O3	0.00	0.00	0.00	0.00	0.01	0.01	0.00	0.00	0.00
MgO	14.18	11.85	13.99	12.11	11.08	11.70	12.53	11.14	13.33
CaO	10.95	9.57	11.11	11.04	10.96	10.80	11.08	11.73	11.53
MnO	0.37	0.30	0.34	0.25	0.24	0.31	0.30	0.26	0.29
FeO	13.64	16.56	13.32	15.41	16.50	16.16	15.18	15.05	13.05
Na2O	1.18	1.34	1.20	1.30	1.49	1.46	1.20	1.34	1.22
K2O	0.15	0.18	0.24	0.26	0.24	0.20	0.23	0.34	0.17
Total	97.07	97.10	97.76	97.39	97.35	97.68	97.42	97.32	97.10

Sample#	DRB-1-60 Relict Igneous core	DRB-1-41 Metamorphic rim	DRB-1-60 Metamorphic rim	DRB-1-60 Metamorphic rim	DRB-1-60 Metamorphic rim	DRB-1-60 Metamorphic rim	PBF-7-108 Meta. amphibole	PBF-7-108 Meta. amphibole	PBF-7-108 Meta. amphibole
SiO2	45.51	46.16	46.57	46.07	47.67	45.59	41.96	42.36	41.69
TiO2	0.36	1.38	1.06	4.03	1.28	2.31	1.00	0.95	0.98
Al2O3	11.85	9.69	9.81	8.93	8.64	10.55	13.66	13.22	13.75
Cr2O3	0.00	0.00	0.00	0.02	0.00	0.01	0.00	0.00	0.08
MgO	11.82	11.43	12.69	12.71	13.59	12.17	9.71	9.77	9.59
CaO	11.22	10.90	11.24	11.12	11.40	11.27	11.66	11.89	11.76
MnO	0.32	0.28	0.29	0.30	0.28	0.31	0.50	0.49	0.47
FeO	14.43	16.10	14.16	12.94	13.54	14.24	16.29	16.79	16.76
Na2O	1.55	1.44	1.33	1.17	1.23	1.31	1.18	1.13	1.18
K2O	0.26	0.24	0.21	0.20	0.21	0.20	1.69	1.60	1.59
Total	97.31	97.62	97.36	97.50	97.83	97.97	97.64	98.19	97.84

Sample#	PBF-7-108 Meta. amphibole	PBF-7-108 Meta. amphibole	PBF-7-108 Meta. amphibole	PBF-7-108 Meta. amphibole	PBF-7-108 Meta. amphibole	PBF-7-108 Metamorphic amphibole	PBF-7-108 Meta. amphibole	PBF-7-108 Meta. amphibole	PBF-7-108 Meta. amphibole
SiO2	42.26	42.16	42.61	43.65	42.62	42.14	42.31	42.51	42.81
TiO2	0.92	0.92	0.79	0.72	0.77	0.97	0.98	0.85	0.88
Al2O3	13.46	13.27	12.79	12.09	13.13	13.69	13.45	13.06	12.76
Cr2O3	0.04	0.02	0.03	0.03	0.05	0.04	0.05	0.01	0.22
MgO	9.48	9.55	9.76	10.23	9.85	9.78	9.84	9.65	9.68
CaO	11.90	11.78	11.85	11.98	11.76	11.92	11.65	11.88	11.82
MnO	0.48	0.50	0.50	0.50	0.47	0.45	0.50	0.51	0.48
FeO	17.05	16.91	17.29	16.78	16.78	16.47	16.32	16.66	16.88
Na2O	1.11	1.09	1.14	1.10	1.12	1.15	1.19	1.05	1.11
K2O	1.58	1.66	1.52	1.32	1.51	1.51	1.75	1.52	1.39
Total	98.28	97.85	98.28	98.40	98.06	98.12	98.05	97.69	98.03

37

Table 1b. Representative plagioclase analyses by electron probe microanalysis.

Sample#	DRB-1-153	DRB-1-153	DRB-1-153	DRB-1-153	DRB-1-153	DRB-1-153	DRB-1-153	DRB-1-153	DRB-1-153	DRB-1-153
Phase	Plagioclase	Plagioclase	Plagioclase	Plagioclase	Plagioclase	Plagioclase	Plagioclase	Plagioclase	Plagioclase	Plagioclase
Rock	Metadiorite	Metadiorite	Metadiorite	Metadiorite	Metadiorite	Metadiorite	Metadiorite	Metadiorite	Metadiorite	Metadiorite
SiO2	66.125	65.898	65.935	66.251	65.782	65.728	64.960	62.564	65.059	62.810
TiO2	0.009	0.016	0.013	0.000	0.005	0.007	0.002	0.024	0.002	0.005
Al2O3	21.323	21.409	21.674	22.221	22.236	21.992	22.604	23.997	21.177	23.597
MgO	0.006	0.001	0.000	0.000	0.000	0.000	0.001	0.002	0.002	0.003
CaO	1.691	1.843	2.185	2.409	2.446	2.547	3.165	3.502	3.527	4.289
FeO	0.133	0.121	0.033	0.028	0.085	0.129	0.035	0.036	1.325	0.179
Na2O	9.976	9.872	9.463	9.626	9.549	9.436	9.142	8.284	9.246	8.624
K2O	0.062	0.074	0.070	0.055	0.055	0.068	0.057	0.747	0.056	0.092
Total	99.327	99.234	99.373	100.590	100.158	99.907	99.966	99.160	100.395	99.599
An	15.72	17.03	20.25	21.60	22.00	22.89	27.59	30.61	29.57	35.31

Sample#	DRB-1-41	DRB-1-41	DRB-1-41	DRB-1-41	DRB-1-41	DRB-1-41	DRB-1-41	DRB-1-41	DRB-1-41	DRB-1-41
Phase	Plagioclase	Plagioclase	Plagioclase	Plagioclase	Plagioclase	Plagioclase	Plagioclase	Plagioclase	Plagioclase	Plagioclase
Rock	Metadiorite	Metadiorite	Metadiorite	Metadiorite	Metadiorite	Metadiorite	Metadiorite	Metadiorite	Metadiorite	Metadiorite
SiO2	61.651	66.679	64.688	64.959	64.187	62.778	62.858	62.955	62.575	62.197
TiO2	0.004	0.022	0.013	0.009	0.011	0.001	0.006	0.010	0.003	0.004
Al2O3	24.590	21.325	22.908	23.038	23.392	24.217	24.112	24.180	24.356	24.514
MgO	0.000	0.004	0.000	0.000	0.000	0.001	0.000	0.000	0.003	0.000
CaO	5.460	1.733	3.388	3.569	3.914	4.773	4.858	5.055	5.232	5.261
FeO	0.036	0.035	0.099	0.099	0.290	0.092	0.105	0.176	0.155	0.036
Na2O	7.929	9.582	8.872	8.686	8.647	8.155	8.235	8.055	8.012	7.997
K2O	0.065	0.076	0.055	0.068	0.062	0.075	0.067	0.073	0.074	0.081
Total	99.749	99.456	100.023	100.440	100.522	100.092	100.241	100.504	100.414	100.090
An	43.08	16.59	29.59	31.12	33.24	39.14	39.34	40.81	41.77	41.94

Sample#	DRB-1-59	DRB-1-59	DRB-1-59	DRB-1-59	DRB-1-59	DRB-1-59	DRB-1-60	DRB-1-60	DRB-1-60	DRB-1-60
Phase	Plagioclase	Plagioclase	Plagioclase	Plagioclase	Plagioclase	Plagioclase	Plagioclase	Plagioclase	Plagioclase	Plagioclase
Rock	Metadiorite	Metadiorite	Metadiorite	Metadiorite	Metadiorite	Metadiorite	Metadiorite	Metadiorite	Metadiorite	Metadiorite
SiO2	63.601	62.770	62.415	62.844	61.986	61.959	62.150	61.547	62.008	61.915
TiO2	0.002	0.011	0.012	0.007	0.000	0.003	0.005	0.006	0.010	0.003
Al2O3	23.320	23.863	23.875	24.064	24.015	24.578	24.470	24.410	24.362	24.431
MgO	0.000	0.001	0.000	0.000	0.000	0.000	0.000	0.000	0.000	0.000
CaO	3.956	4.515	4.649	4.725	4.797	5.253	5.289	5.303	5.341	5.423
FeO	0.044	0.054	0.310	0.039	0.038	0.060	0.027	0.075	0.039	0.030
Na2O	8.686	8.447	8.287	8.198	8.294	7.922	7.874	7.840	7.677	7.667
K2O	0.088	0.067	0.075	0.069	0.068	0.076	0.081	0.069	0.051	0.068
Total	99.697	99.736	99.623	99.946	99.200	99.851	99.896	99.250	99.488	99.537
An	33.34	37.02	38.13	38.78	38.87	42.14	42.44	42.64	43.36	43.73

Table 1b. Representative plagioclase analyses by electron probe microanalysis.

Sample#	DRB-1-60	DRB-1-60	PBF-7-108	PBF-7-108	PBF-7-108	PBF-7-108	PBF-7-108	PBF-7-108	PBF-7-108
Phase	Plagioclase	Plagioclase	Plagioclase	Plagioclase	Plagioclase	Plagioclase	Plagioclase	Plagioclase	Plagioclase
Rock	Metadiorite	Metadiorite	Metagrano-diorite	Metagrano-diorite	Metagrano-diorite	Metagrano-diorite	Metagrano-diorite	Metagrano-diorite	Metagrano-diorite
SiO2	62.173	61.765	59.921	60.720	60.386	60.290	59.946	60.192	60.226
TiO2	0.000	0.002	0.005	0.000	0.021	0.014	0.016	0.022	0.016
Al2O3	24.718	24.465	25.833	25.543	25.525	25.720	25.959	26.031	25.653
MgO	0.001	0.009	0.000	0.000	0.003	0.000	0.000	0.000	0.000
CaO	5.504	5.527	6.775	6.825	6.889	6.957	6.974	7.010	7.011
FeO	0.105	0.019	0.037	0.056	0.050	0.093	0.065	0.038	0.046
Na2O	7.145	7.730	7.096	7.023	7.044	7.072	6.951	7.045	6.965
K2O	0.063	0.069	0.036	0.230	0.210	0.083	0.073	0.081	0.194
Total	99.719	99.591	99.711	100.434	100.144	100.252	99.992	100.422	100.111
An	45.84	44.00	51.26	51.25	51.46	51.90	52.41	52.19	52.21

Sample#	PBF-7-108	PBF-7-159	PBF-7-169	PBF-7-108	PBF-7-108	PBF-7-108	PBF-7-108	PBF-7-108	PBF-7-108
Phase	Plagioclase	Plagioclase	Plagioclase	Plagioclase	Plagioclase	Plagioclase	Plagioclase	Plagioclase	Plagioclase
Rock	Metagrano-diorite	Metagrano-diorite	Pinked	Metagrano-diorite	Metagrano-diorite	Metagrano-diorite	Metagrano-diorite	Metagrano-diorite	Metagrano-diorite
SiO2	59.678	65.648	68.634	61.994	61.176	60.872	60.780	60.195	59.656
TiO2	0.003	0.014	0.003	0.000	0.000	0.000	0.000	0.014	0.000
Al2O3	26.159	22.596	20.228	24.763	25.433	25.735	25.494	25.736	26.104
MgO	0.000	0.006	0.000	0.013	0.008	0.008	0.000	0.004	0.000
CaO	7.323	2.964	0.537	1.318	6.305	6.606	6.733	7.032	7.082
FeO	0.213	0.035	0.021	0.165	0.060	0.056	0.026	0.162	0.108
Na2O	6.851	9.188	9.686	5.531	7.217	7.113	7.104	7.098	6.874
K2O	0.125	0.109	0.102	5.741	0.183	0.315	0.087	0.066	0.111
Total	100.364	100.560	99.211	99.546	100.382	100.719	100.224	100.310	99.935
An	53.86	26.13	5.74	13.53	48.71	49.94	50.96	52.11	52.98

Sample#	PBF-7-159	PBF-7-159	PBF-7-159	PBF-7-169	PBF-7-169	PBF-7-169	PBF-7-169	PBF-7-169	PBF-7-169
Phase	Plagioclase	Plagioclase	Plagioclase	Plagioclase	Plagioclase	Plagioclase	Plagioclase	Plagioclase	Plagioclase
Rock	Metagrano-diorite	Metagrano-diorite	Metagrano-diorite	Pinked	Pinked	Pinked	Pinked	Pinked	Pinked
SiO2	63.981	64.560	64.051	69.527	69.351	69.721	69.190	69.867	69.801
TiO2	0.000	0.002	0.000	0.004	0.006	0.013	0.007	0.009	0.000
Al2O3	22.764	23.482	23.596	19.815	19.889	19.730	20.136	20.062	19.972
MgO	0.000	0.000	0.000	0.000	0.000	0.000	0.000	0.000	0.002
CaO	3.542	3.932	4.146	0.434	0.438	0.455	0.468	0.484	0.489
FeO	0.022	0.046	0.056	0.040	0.061	0.079	0.102	0.064	0.122
Na2O	9.043	8.615	8.484	9.739	9.784	9.868	10.026	9.503	9.627
K2O	0.080	0.103	0.089	0.098	0.094	0.076	0.102	0.098	0.112
Total	99.432	100.740	100.429	99.678	99.657	100.046	100.043	100.200	100.136
An	30.09	33.36	34.91	4.66	4.69	4.83	4.88	5.30	5.28

Table 2. Whole Rock Major and trace element analyses by X-ray fluorescence spectrometry.

	DRB Plutonic Suite											
Core#	DRB1	DRB1	DRB1	DRB1	DRB1	DRB1	DRB1	DRB1	DRB1	DRB1	DRB1	DRB1
Box	18	22	25	41	51	59	60	98	99	124	153	156
Sample#	1005	1028	1047	1151	1215	1268	1276	1504	1509	1660	1837	1852
Rock Type	Quartz Diorite	Tonalite	Diorite	Quartz Diorite	Quartz Diorite	Quartz Diorite	Tonalite	Tonalite	Quartz Diorite	Quartz Diorite	Quartz Diorite	Quartz Diorite
SiO2	60.04	69.38	50.00	54.34	59.58	53.50	70.37	70.04	55.58	58.46	57.55	59.48
TiO2	0.78	0.53	1.09	1.17	0.76	1.05	0.58	0.60	0.65	0.96	0.71	0.79
Al2O3	17.05	15.16	17.39	16.14	17.65	17.69	15.10	15.31	18.15	17.63	17.46	17.51
Fe2O3	8.05	5.66	12.10	12.08	5.77	10.37	3.61	3.65	8.22	9.11	8.22	7.47
MnO	0.15	0.08	0.20	0.15	0.13	0.18	0.05	0.06	0.14	0.11	0.13	0.12
MgO	3.15	1.25	6.72	4.25	2.17	3.77	1.00	1.07	4.99	2.74	4.15	2.62
CaO	5.89	3.41	9.60	8.37	5.94	8.26	3.22	2.94	9.24	4.71	6.06	6.92
Na2O	4.28	5.06	3.84	3.21	5.67	4.69	6.78	7.04	3.94	7.93	6.21	4.54
K2O	0.93	0.53	0.47	1.03	0.93	0.26	0.29	0.29	0.22	0.13	0.66	0.79
P2O5	0.18	0.11	0.14	0.16	0.23	0.25	0.15	0.17	0.13	0.14	0.11	0.21
SUM	100.49	101.18	101.56	100.91	98.82	100.03	101.15	101.17	101.26	101.92	101.25	100.44
%LOI	1.51%	1.07%	1.50%	0.69%	0.47%	0.75%	1.33%	0.55%	0.79%	1.86%	0.46%	0.54%
Nb	7	8	3	5	6	6	4	11	10	5	4	6
Zr	141	171	65	107	181	91	85	202	213	151	84	149
Y	25	25	18	27	22	24	16	30	31	22	21	22
Sr	316	236	263	297	373	403	381	225	213	179	199	407
Rb	19	9	7	20	18	4	3	4	5	0	11	16
Zn	81	33	91	69	85	72	59	24	22	52	55	39
Cu	81	115	87	26	7	80	6	2	6	12	71	62
Ni	12	3	41	6	7	7	24	2	1	12	28	10
Cr	16	6	142	19	9	13	22	1	1	8	16	5
Sc	15	12	38	30	16	25	24	11	12	20	25	15
V	142	42	316	352	99	228	172	43	40	184	188	144
Ba	579	170	126	346	442	156	106	245	187	64	222	327

Major elements analyzed on pre-ignited, fused glass beads. Major element results in weight % oxide.
Trace elements analyzed on pressed powder pellets with polyvinyl alcohol binding. Trace elements in ppm by weight.

42

Table 2. Whole Rock Major and trace element analyses by X-ray fluorescence spectrometry.

	PBF Plutonic Suite: "Unpinked"							PBF Plutonic Suite: "Partly Pinked"			
Core#	PBF7	PBF7	PBF7	PBF7	PBF7	PBF7	PBF7	PBF7	PBF7	PBF7	PBF7
Box	103	107	108	115	115T	139	159	143	145	157	157
Sample#	2550	2602	2629	2726	2726	3086	3387	3139.6	3177	3352	3355
Rock Type	Grano-diorite	Grano-diorite	Grano-diorite	Grano-diorite	Grano-diorite	Grano-diorite	Grano-diorite	part pinked granite	part pinked granite	part pinked granite	part pinked granite
SiO2	58.16	54.69	64.24	58.36	62.22	59.30	68.36	71.57	72.29	72.78	72.54
TiO2	1.39	1.76	1.07	1.13	0.84	0.83	0.84	0.51	0.55	0.51	0.53
Al2O3	16.74	16.54	15.66	15.53	15.29	17.54	14.39	14.06	13.34	13.53	13.62
Fe2O3	8.46	9.93	6.18	7.69	6.85	8.37	5.08	3.50	3.64	3.46	3.67
MnO	0.15	0.18	0.12	0.14	0.12	0.18	0.09	0.07	0.06	0.09	0.06
MgO	3.46	3.52	1.97	4.48	3.90	2.97	1.42	0.56	0.65	0.52	0.59
CaO	6.94	7.69	4.70	7.22	5.69	5.82	4.62	1.68	2.00	2.17	2.00
Na2O	3.93	2.84	3.90	3.49	3.52	4.11	3.29	3.58	3.36	3.72	3.57
K2O	1.48	3.15	3.22	1.29	2.25	1.69	2.19	5.00	4.52	3.89	4.14
P2O5	0.34	0.60	0.21	0.24	0.17	0.13	0.17	0.11	0.11	0.11	0.11
SUM	101.06	100.90	101.27	99.57	100.84	100.97	100.45	100.63	100.52	100.78	100.84
%LOI	1.60%	1.26%	0.63%	2.28%	1.89%	1.78%	1.36%	0.85%	0.71%	1.05%	1.36%
Nb	19	18	23	10	8	5	4	24	27	25	25
Zr	275	305	298	172	138	134	122	242	268	238	259
Y	42	53	44	22	19	21	33	57	58	59	56
Sr	421	347	311	450	388	341	551	135	147	152	138
Rb	49	97	70	42	69	55	39	104	98	80	79
Zn	179	89	66	69	63	103	96	50	57	53	57
Cu	81	117	51	32	19	61	52	3	8	51	12
Ni	19	22	14	52	52	21	10	5	5	8	7
Cr	42	32	12	86	73	47	30	0	3	0	0
Sc	20	24	11	22	19	17	22	4	8	5	2
V	157	147	96	147	114	148	162	31	31	31	30
Ba	486	995	960	378	852	427	393	803	851	766	821

Major elements analyzed on pre-ignited, fused glass beads. Major element results in weight % oxide.
Trace elements analyzed on pressed powder pellets with polyvinyl alcohol binding. Trace elements in ppm by weight.

Table 2. Whole Rock Major and trace element analyses by X-ray fluorescence spectrometry.

	PBF Plutonic Suite: "Pinked"											
Core#	C10A	PBF7	PBF7	PBF7	PBF7	PBF7	PBF7	SA	SA	SA	SA	SA
Box	none	167	169	171	171	173	165	56	57	58	61	62
Sample#	1734	3503	3541	3568	3570	3593	3467	1078	1086	1089	1107	1118
Rock Type	pink granite	pink granite	pink granite	pink granite	pink granite	pink granite	pink granite	pink granite	pink granite	pink granite	pink granite	pink granite
SiO2	74.16	77.12	75.45	75.31	76.84	74.62	71.90	74.66	71.95	73.69	74.15	72.72
TiO2	0.35	0.06	0.08	0.14	0.09	0.11	0.49	0.24	0.26	0.21	0.25	0.24
Al2O3	13.93	12.66	13.00	13.23	12.96	12.71	13.31	14.22	15.58	13.56	14.20	13.72
Fe2O3	2.39	1.12	1.54	1.36	1.30	1.48	3.34	1.86	1.89	1.37	1.89	1.74
MnO	0.06	0.02	0.07	0.04	0.03	0.04	0.07	0.04	0.03	0.04	0.05	0.04
MgO	0.45	0.02	0.11	0.28	0.07	0.07	0.55	0.50	0.62	0.48	0.75	0.65
CaO	0.81	0.49	0.88	0.98	0.59	0.59	1.82	1.13	1.21	1.05	1.81	1.38
Na2O	3.82	4.39	5.63	4.03	3.90	4.11	3.54	3.16	3.75	3.36	3.40	3.20
K2O	4.89	4.79	3.17	5.25	5.25	5.03	4.79	4.52	5.08	4.54	4.14	4.69
P2O5	0.08	0.01	0.02	0.02	0.02	0.02	0.11	0.06	0.07	0.05	0.06	0.06
SUM	100.94	100.67	99.93	100.64	101.04	98.78	99.92	100.38	100.44	98.36	100.70	98.43
%LOI	0.71%	0.71%	0.84%	0.71%	0.51%	0.29%	0.37%	1.20%	0.93%	0.60%	1.17%	0.79%
Nb	34	143	7	40	52	27	24	13	16	14	13	10
Zr	215	138	95	115	120	130	207	131	143	124	125	134
Y	29	114	28	82	80	51	48	18	21	12	24	12
Sr	123	6	716	27	21	20	121	172	183	186	223	261
Rb	183	143	21	106	97	98	127	194	215	198	153	146
Zn	51	53	138	34	37	48	50	11	12	12	20	15
Cu	1	0	41	0	0	0	5	2	8	1	0	2
Ni	5	2	11	5	2	3	5	9	5	4	5	8
Cr	0	0	37	0	0	0	0	24	3	0	0	3
Sc	2	4	32	4	2	5	6	2	5	3	2	3
V	17	0	356	3	3	0	26	17	22	13	17	23
Ba	798	4	157	115	85	66	844	719	840	800	892	1843

Major elements analyzed on pre-ignited, fused glass beads. Major element results in weight % oxide.
Trace elements analyzed on pressed powder pellets with polyvinyl alcohol binding. Trace elements in ppm by weight.

Table 3. Whole rock REE, Y, Pb, Th, and U analyses by ICP-MS.

Core	DRB1	DRB1	DRB1	DRB1	PBF7	PBF7	PBF7	PBF7	PBF7	C5	C5
Box	18	25	41	60	171	103	107	108	139	none	none
Sample#	1005	1047	1151	1276	3568	2550	2602	2629	3086	1084	1080
	quartz diorite	diorite	quartz diorite	tonalite	pink granite	grano-diorite	grano-diorite	grano-diorite	grano-diorite	pink granite	felsic dike
La ppm	10.4	3.6	7.9	6.5	17.0	25.8	29.8	22.2	11.3	11.7	32.4
Ce	25.7	9.6	21.7	15.5	48.2	63.7	69.4	51.1	28.3	26.2	79.8
Pr	3.2	1.3	3.3	1.9	7.2	8.6	8.6	5.8	3.9	3.2	10.3
Nd	13.1	5.5	14.1	7.5	26.8	32.6	34.2	22.7	15.1	13.5	38.2
Sm	2.9	1.4	4.1	1.8	8.3	7.6	9.0	5.4	4.3	10.3	10.3
Eu	0.60	0.39	0.92	0.43	0.34	1.77	2.54	1.30	1.05	4.69	2.08
Gd	3.3	2.0	4.1	2.2	9.9	7.2	7.9	5.5	3.6	3.7	8.7
Tb	0.59	0.38	0.72	0.42	2.05	1.25	1.48	1.19	0.62	0.76	1.50
Dy	3.2	2.1	4.3	2.4	11.3	6.9	8.0	6.4	3.4	4.1	8.1
Ho	0.64	0.45	0.84	0.53	2.19	1.34	1.80	1.52	0.69	0.96	1.59
Er	2.1	1.4	2.5	1.8	6.9	4.0	4.6	4.2	2.2	2.5	5.1
Tm	0.37	0.24	0.39	0.25	1.02	0.57	0.68	0.66	0.36	0.39	0.72
Yb	1.8	1.3	2.0	1.6	5.4	3.1	3.6	3.4	1.7	2.0	3.9
Lu	0.28	0.20	0.31	0.27	0.80	0.48	0.59	0.58	0.31	0.30	0.61
Y	26.5	19.6	27.8	14.5	82.5	42.1	46.5	40.7	24.4	24.7	58.8
Pb	4.5	3.9	16.6	3.4	14.1	16.6	12.7	13.0	14.8	19.8	18.9
Th	0.6	0.4	0.9	1.8	1.4	1.4	4.4	6.9	1.0	4.5	2.1
U	0.6	0.4	0.9	0.4	1.4	1.4	1.4	1.5	1.0	1.6	2.1
La /chondrite	30.6	10.6	23.4	19.2	49.9	75.8	87.7	65.3	33.4	34.4	95.3
Ce	28.3	10.6	23.8	17.1	52.9	70.0	76.3	56.1	31.1	28.7	87.6
Pr	26.6	10.8	26.9	16.0	59.2	70.8	70.9	48.3	32.1	26.7	85.1
Nd	22.6	9.5	24.2	12.9	46.2	56.2	59.0	39.2	26.1	23.3	65.9
Sm	14.8	7.2	20.9	9.0	42.5	39.1	46.2	27.8	22.2	52.7	52.8
Eu	8.2	5.3	12.5	5.9	4.6	24.2	34.7	17.7	14.3	64.0	28.5
Gd	13.0	7.9	16.0	8.7	38.9	28.2	31.2	21.7	14.0	14.4	34.0
Tb	12.4	8.0	15.2	8.9	43.1	26.4	31.2	25.1	13.0	16.0	31.7
Dy	11.3	7.4	15.0	8.5	39.8	24.4	28.2	22.4	11.9	14.4	28.4
Ho	8.2	5.7	10.7	6.7	28.1	17.2	23.1	19.4	8.9	12.3	20.4
Er	10.8	7.2	12.9	9.5	35.2	20.3	23.8	21.5	11.3	12.9	26.0
Tm	11.4	7.5	12.1	7.8	32.0	17.9	21.2	20.6	11.1	12.2	22.4
Yb	8.9	6.5	10.2	7.8	27.1	15.7	18.0	16.8	8.6	10.0	19.7
Lu	8.2	5.9	9.0	7.9	23.5	14.1	17.5	17.2	9.2	8.9	18.0
Y	12.6	9.4	13.2	6.9	39.3	20.0	22.1	19.4	11.6	11.8	28.0